AGU ADVANCING EARTH AND SPACE SCIENCES

JGR Atmospheres

RESEARCH ARTICLE

10.1029/2023JD039113

Key Points:

- The sub-grid Turbulent Orographic Form Drag (TOFD) parameterization scheme has been applied into Regional Climate Model version 4 (RegCM4)
- The TOFD scheme improves the ability of RegCM4 in reproducing the atmospheric circulation
- The TOFD scheme considerably enhances the performance of RegCM4 in simulating the monsoonal precipitation over China in summer

Correspondence to:

A. Huang,
anhuang@nju.edu.cn

Citation:

Gu, C., Huang, A., Li, X., Yang, B., Zhou, X., & Wu, Y. (2023). Impact of sub-grid turbulent orographic form drag on the summer monsoon precipitation simulation over China. *Journal of Geophysical Research: Atmospheres*, *128*, e2023JD039113. https://doi.org/10.1029/2023JD039113

Received 19 APR 2023
Accepted 22 SEP 2023

Author Contributions:

Conceptualization: Chunlei Gu, Anning Huang
Data curation: Chunlei Gu, Anning Huang
Formal analysis: Chunlei Gu, Anning Huang, Xin Li, Ben Yang
Investigation: Chunlei Gu, Anning Huang, Yang Wu
Methodology: Chunlei Gu, Anning Huang, Xu Zhou
Resources: Chunlei Gu, Anning Huang
Software: Chunlei Gu, Anning Huang, Xu Zhou, Yang Wu
Supervision: Chunlei Gu, Anning Huang
Validation: Chunlei Gu, Anning Huang, Xin Li, Ben Yang, Yang Wu
Visualization: Chunlei Gu, Anning Huang
Writing – original draft: Chunlei Gu, Anning Huang, Xin Li
Writing – review & editing: Chunlei Gu, Anning Huang, Xin Li, Ben Yang, Xu Zhou, Yang Wu

Impact of Sub-Grid Turbulent Orographic Form Drag on the Summer Monsoon Precipitation Simulation Over China

Chunlei Gu[1], Anning Huang[1,2], Xin Li[3], Ben Yang[1], Xu Zhou[4], and Yang Wu[3]

[1]School of Atmospheric Sciences, Nanjing University, Nanjing, China, [2]Qinghai Lake Comprehensive Observation Research station, Chinese Academy of Sciences, Gangcha, China, [3]Nanjing Joint Institute for Atmospheric Sciences & Key Laboratory of Transportation Meteorology of CMA, Chinese Academy of Meteorological Sciences - Jiangsu Meteorological Service, Nanjing, China, [4]National Tibetan Plateau Data Center, State Key Laboratory of Tibetan Plateau Earth System, Environment and Resources, Institute of Tibetan Plateau Research, Chinese Academy of Sciences, Beijing, China

Abstract Terrain has multi-scale dynamic impacts on the climate. The Regional Climate Model version 4 (RegCM4) has simulation uncertainty partly due to insufficient description of sub-grid orographic drag (SOD). In this study, the sub-grid turbulent orographic form drag (TOFD) scheme has been adopted into the RegCM4 to better describe SOD. Results show that the overestimated near surface wind over rugged areas leads to non-negligible biases of the summer monsoon precipitation simulation over China in the original RegCM4, whose skill in simulating the summer precipitation over the monsoonal regions of China can be remarkably improved by adopting the sub-grid TOFD scheme. Compared to the original RegCM4, the Taylor scores (root mean square error) of the precipitation simulated by the RegCM4 with the sub-grid TOFD scheme are increased (decreased) by 4%, 13%, 11%, and 7% (8%, 5%, 30%, and 16%) over the southeastern China, the mid-lower Yangtze River Basin, the Huang-Huai Basin, and the northeastern China, respectively. The improved precipitation simulation mainly comes from the atmospheric circulation simulation improved by adopting the sub-grid TOFD scheme, which leads to cyclonic (anti-cyclonic) wind differences over the southeastern (northeastern) China from the boundary layer to the mid-troposphere and thereafter vertical motion differences in the middle troposphere, further resulting in the variation of the simulated precipitation intensity (heavy to torrential) and the convective precipitation and consequential improvement of summer monsoon precipitation simulation. This study indicates that the dynamic impact of micro-scale terrain plays an important role in the summer monsoon precipitation simulation.

Plain Language Summary The description of mechanical effects of the sub-grid scale terrain in the numerical model is important to the climate modeling. This study introduces the Sub-grid Turbulent Orographic Form Drag (TOFD) parameterization scheme into the Regional Climate Model version 4 (RegCM4). The TOFD scheme offers the RegCM4 a description of the turbulent drag on the air flow induced by the sub-grid terrain and reduces the large bias of the near surface wind simulated by the original RegCM4 over the areas with the complex terrain in China. The RegCM4 with the TOFD scheme performs better in simulating the precipitation over eastern China in summer relative to the original RegCM4. This study not only further improves the capability of RegCM4 in simulating summer precipitation over the monsoonal region of China, but also illustrates the essential role of the turbulent orographic form drag in the formation of regional climate.

1. Introduction

Rugged terrain covers most of the land surface in Earth and has various thermal and dynamic effects on weather and climate (Barry, 2008). Under the influence of terrain elevation, shading, and land cover, the surface temperature of rugged area presents strong heterogeneity which impacts the thermal stratification of the overlying atmosphere (Gu et al., 2022; Shi et al., 2019; Wu et al., 2016). Orographic mechanical effects (OME) on synoptic systems depend on the scale of topography and air flow (R. Zhang et al., 2020). The macro-scale ($\Delta L \sim 10^3$ km) mountain ranges with the horizontal scale of $\sim 10^3$ km force the planetary waves (Charney & Eliassen, 1949; Davis, 1997; McHall, 1991; Yeh, 1950). The meso-scale ($\Delta L \sim 10^1$–10^2 km) mountain blocks the weak low-level airflow, lifts the stronger airflow, and produces orographic gravity wave (Athanassiadou, 2003; Xu et al., 2021; Zadra et al., 2003). The micro-scale ($\Delta L \leq 10^0$ km) topography drags the airflow by forming the turbulent (Belcher & Wood, 1996; Zhou et al., 2019).

The multi-scale OME on the air flow greatly affect the atmospheric stratification, water vapor transport, cloud micro-physical structures, and thereafter precipitation over the mountains and downstream areas (R. B. Smith, 2019; Y. Wang et al., 2020; M. Yang et al., 2007; Zagrodnik et al., 2019; Y. Zhao et al., 2020). Previous studies have shown that the topography has significant influence on the amount, intensity, phase, and spatial-temporal distribution of precipitation (Singh & Kumar, 1997; Anders et al., 2008; Feng & Zhou, 2012; Y. Zhang et al., 2014; Garvert et al., 2007). Therefore, reasonable representation of OME is crucial for precipitation modeling over the mountains and adjacent areas (Cannon et al., 2017; S. Chen et al., 2019; Lee et al., 2015).

Efforts to better describe the OME in numerical models have been made as follows: (a) Increasing the horizontal resolution of grid-scale topography to enhance the depiction of grid scale OME (Li et al., 2022; C. Zhao et al., 2019; Gao et al., 2006). By raising the horizontal resolution to tens of (or several) kilometers, the numerical models come to well characterize the macro-scale (meso-scale) OME but leave the micro-scale OME unresolved (S. A. Smith et al., 2006; Vosper et al., 2020; Lin et al., 2018; van Niekerk et al., 2016). (b) Take account the sub-grid scale orographic variation by the "envelope orography" and "effective roughness length" (Fiedler & Panofsky, 1972; Wallace et al., 1983; Wood & Mason, 1993). The "envelope orography" ("effective roughness length") represents the meso-scale (micro-scale) sub-grid orographic drag (SOD) to a certain degree but has ineluctable disadvantages due to the lack of physical basis (Koo et al., 2018; Lott & Miller, 1997; Slingo & Pearson, 1987; Zhou et al., 2019). (c) Thus, it has become common to develop the parameterization schemes directly describing the SOD such as the gravity wave drag, the flow-blocking drag, and the turbulent orographic form drag (TOFD) (Beljaars et al., 2004; Choi & Hong, 2015; Kim & Doyle, 2005; McFarlane et al., 1986; Xu et al., 2019). Challenges remain in the development of the SOD parameterization. Lots of previous SOD parameterization schemes are developed based on the assumption of isotropic SOD and nowadays a new generation of the anisotropic SOD parameterization are developed considering the 3-dimensional anisotropic variation of the terrain and the SOD (van Niekerk et al., 2023; Xie et al., 2020; Xue & Shen, 2023). Another Challenge is to make the SOD parameterization more "scale aware" (van Niekerk & Vosper, 2021).

The adoptions of SOD parameterization improve the ability of models in precipitation forecast through better description of the sub-grid OME (R. Zhang et al., 2020; Y. Wang et al., 2020; Zhong & Chen, 2015; Lee et al., 2015; Xue et al., 2021). Insufficient description of the SOD maintains an important source of model uncertainty (Elvidge et al., 2019; van Niekerk et al., 2020). The global climate models (GCMs) commonly underestimate (overestimate) precipitation over the southeastern China (Tibetan Plateau, TP) (Jiang et al., 2020; Kusunoki, 2018; Tong et al., 2022; Jiang et al., 2016; Xin et al., 2020; Alapaty et al., 2012; H. Chen et al., 2010; C. Zhao et al., 2020; Scinocca et al., 2016). The simulated precipitation biases of the GCMs can be clearly reduced by adopting the high-resolution regional climate models (RCMs) (Gao et al., 2013; Gao et al., 2011; Yu et al., 2010; Bao et al., 2015; H. Yang et al., 2016; Ma et al., 2015; L. Zou & Zhou, 2017). However, the problem of dry (wet) bias over the southeastern China (TP) remains in the RCMs, such as the Regional Climate Model Version 4 (RegCM4) (Nguyen-Xuan et al., 2022; Giorgi et al., 2012; Gao et al., 2017; Lu et al., 2019; M. Yang et al., 2018; J. Zou & Xie, 2012; Shi et al., 2018; J. Chen et al., 2014). Studies indicate that the Weather Research and Forecasting Model (WRF) outperforms the RegCM4 in down-scaling precipitation over China (Ge et al., 2021; Huang & Gao, 2018; Liang et al., 2019), which can be partly attributed to the differences of the abilities of the WRF and RegCM4 in the description of the SOD (R. Zhang et al., 2020; Zhou et al., 2017; Liang et al., 2012).

Improving the simulation of regional climate over the mountainous areas is one of the original goals and usual applications of RCMs (Giorgi & Bates, 1989; Boroneant et al., 2006; Torma et al., 2011; X. Wang et al., 2016). The development of RCMs has come to a horizontal resolution of several kilometers recently, resulting in detailed grid-scale description of meso-scale orographic drag (Becker & Vadas, 2018; Coppola et al., 2021; Kendon et al., 2017; Prein et al., 2015; Schär et al., 2020). However, the TOFD parameterization has added value to the WRF even with a horizontal resolution of ~3 km (Y. Wang et al., 2020), suggesting that the TOFD scheme is still necessary for the weather modeling over rugged areas even at very high model resolution. Previous studies show that the TOFD scheme enhances the ability of the WRF in simulating precipitation over the southeastern China and part of the Himalaya (Y. Wang et al., 2020; Xue et al., 2021). But these studies mainly discuss about the skills of weather forecast or specific weather case based on the numerical experiments with relatively small domain and short simulation period. The effects of the TOFD scheme on the simulation of the summer precipitation climatology over China remain inadequately elucidated.

10.1029/2023JD039113

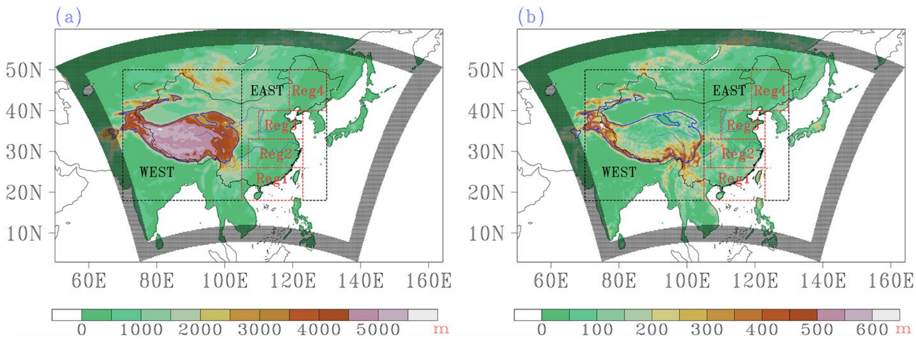

Figure 1. Grid-scale elevation (a) and standard deviation of filtered elevation σ_{flt} (b) in the model domain with the horizontal resolution of 25 km. The thick blue lines are the elevation contour of 3,000 m. The thin blue lines indicate the Yangtze River and the Yellow River. The red dash rectangles show the sub-regions Reg1, Reg2, Reg3, and Reg4. The black dash rectangles show the west and east sub-regions. The black grids illustrate the lateral buffer zone.

Two questions are raised: (a) Can the TOFD parameterization scheme improve the ability of the RegCM4 with a horizontal resolution of tens of kilometers in simulating the precipitation over China? (b) How does the TOFD parameterization scheme influence the ability of RegCM4 in simulating the precipitation? In this study, the TOFD scheme has been introduced into the RegCM4 and its impacts on the model performance in simulating the summer monsoon precipitation over China have been investigated. Section 2 introduces the TOFD scheme, RegCM4, data, and methodology. The effects of TOFD scheme on modeling the summer precipitation over China are illustrated in Section 3. Section 4 discusses the possible physical mechanisms. Conclusion and discussion are given in Section 5.

2. TOFD Scheme, RegCM4, Data and Methodology

2.1. The TOFD Parameterization Scheme

The sub-grid TOFD scheme (Beljaars et al., 2004) calculates the TOFD caused by the micro-scale topography based on the method of Wood et al. (2001). The grid-scale TOFD at each vertical layer is estimated by Equation 1 and accounted in the atmospheric equation:

$$\frac{\partial}{\partial z}\left(\frac{\tau_o}{\rho}\right) = -1.08372058\times10^{-7}\cdot|\vec{V}|\cdot\vec{V}\cdot e^{-(z/1500)^{1.5}}\cdot\sigma_{flt}^2\cdot z^{-1.2} \quad (1)$$

where e, τ_o, z, ρ, $|\vec{V}|$, and $\vec{V}$ are the natural constant, stress in the wind direction, elevation above ground surface, air density, wind speed, and horizontal wind vector at each layer. $\vec{V}$ has zonal (meridional) component $u(v)$. $|\vec{V}|$ is calculated by $|\vec{V}| = \sqrt{u^2 + v^2}$. σ_{flt} is the standard deviation of the filtered sub-grid terrain elevation. The value of the TOFD is determined by σ_{flt}^2, $\vec{V}$, and z. The TOFD increases with the raising σ_{flt}^2 and $\vec{V}$ but exponentially decreases with the raising z. Following Xue et al. (2021), σ_{flt} at each model grid in this study is derived from the $30'' \times 30''$ (~1 km×~1 km) Global Multi-resolution Terrain Elevation Data (GMTED, Danielson & Gesch, 2011). Details about the TOFD scheme and the method for calculating σ_{flt} are shown in Beljaars et al. (2004) and Xue et al. (2021). As shown in Figure 1, the large values of σ_{flt} over the western TP, Himalaya, and Hengduan Mountain indicate the complex micro-scale terrain and strong TOFD.

2.2. RegCM4

The RegCM as the first limited-area model for regional climate simulation has been developed since the late 1980s (Dickinson et al., 1989; Giorgi, 1990). After more than 30 years of intensive development in dynamic cores, physical process descriptions, portability, and user-friendliness, the RegCM has reached its fifth generation recently (RegCM5, details in Pal et al., 2007; Giorgi et al., 1993; Giorgi et al., 2012; Coppola et al., 2021; Giorgi et al., 2023). The Abdus Salam International Centre for Theoretical Physics (ICTP) establishes the RegCM with public free release (https://github.com/ictp-esp/RegCM), abundant supporting data (http://clima-dods.ictp.it/regcm4), and convenient user communication platform (https://lists.ictp.it/mailman/listinfo/regcnet), which

10.1029/2023JD039113

Table 1
Model Configuration

Name	Value
Dynamical Core	Hydrostatical Core (Grell et al., 1994)
Cumulus Scheme	Tiedtke (Tiedtke, 1996) over the landKain-Fritsch (Kain & Fritsch, 1990) over the ocean
Planetary Boundary Layer Scheme	Holtslag (Holtslag et al., 1990)
Moisture Scheme	SUBEX (Pal et al., 2000)
Land Surface Model	CLM4.5 (Oleson et al., 2013)
Radiation Transfer Model	CCM3 (Kiehl et al., 1998)
Ocean Flux Scheme	Zeng (Zeng et al., 1998)
Lateral Boundary Condition Scheme	Relaxation Exponential Technique (Buffer zone shown in Figure 1)
Oceanic Surface Condition	1° × 1° NOAA OISST (Reynolds et al., 2002)
Atmospheric Condition	1.5° × 1.5° ERA-Interim Reanalysis (Dee et al., 2011)
Grid-scale Topography	30″ × 30″ GMTED (Danielson & Gesch, 2011)
Initial Soil Moisture	0.25° × 0.25° ESA CCI Surface Soil Moisture Combined Product (Dorigo et al., 2021)

benefits a great deal to the geophysical research community (Pan et al., 2020; Sawadogo et al., 2021; Teodoro et al., 2021; Torres-Alavez et al., 2021). Compared to the RegCM4, the main progresses of the RegCM5 are some additional physical schemes and a new non-hydrostatic dynamic core (Giorgi et al., 2023). The performances of the new core and schemes of the RegCM5 have not been well evaluated while the RegCM4 are widely applied in the studies over East Asia (Gao & Giorgi, 2017; Lu et al., 2019; Xie et al., 2021). Therefore, the RegCM4 is adopted in this study.

2.3. Numerical Experimental Design

Two experiments named as the SEXP and CTRL experiments are conducted by the hydro-static RegCM4 and the only difference between them is with or without the sub-grid TOFD scheme. Following Niu et al. (2021), the model domain covers East Asia with the resolution of 25 km (Figure 1), which owns 320 (240) zonal (meridional) grids and centers at (34°N, 107°E). The model has 23 vertical layers. The top layer reaches 50 hPa.

The integration is conducted from 1 May to 31 August in each year from 2006 to 2015 with the time step of 30 s in the dynamic core. The land surface process, emission-absorption of cloud and gas particles, convection, and solar radiation are calculated every 10 min, 1 hr, 30 s, and 10 min. The lateral boundary condition updates every 6 hr. The model results are output every 24 hr in each experiment. Simulations in May are discarded as the model spin-up (C. Gu et al., 2022). Only the simulations in boreal summer (Jun, July, and August) are used for analysis. The physical packages and forcing data adopted in the experiments are listed in Table 1.

2.4. Data for Model Evaluation

To evaluate the model performance and investigate the related physical mechanisms, the following data are used:

1. The daily precipitation data from Asian Precipitation Highly-Resolved Observational Data Integration Toward Evaluation (APHRODITE, Yatagai et al., 2012) with the horizontal resolution of 0.25° × 0.25° in summers of 2006–2015.
2. The hourly ERA5 Atmospheric Reanalysis with the horizontal resolution of 0.25° × 0.25° at 37 vertical levels (Hersbach et al., 2020) in summers of 2006–2015.

2.5. Methodology

Following Qian et al. (2007), the daily precipitation (R) is classified as the light (0.1 mm·d^{-1} $\leq R <$ 10.0 mm·d^{-1}), moderate (10.0 mm·d^{-1} $\leq R <$ 25.0 mm·d^{-1}), heavy (25.0 mm·d^{-1} $\leq R <$ 50.0 mm·d^{-1}), and torrential

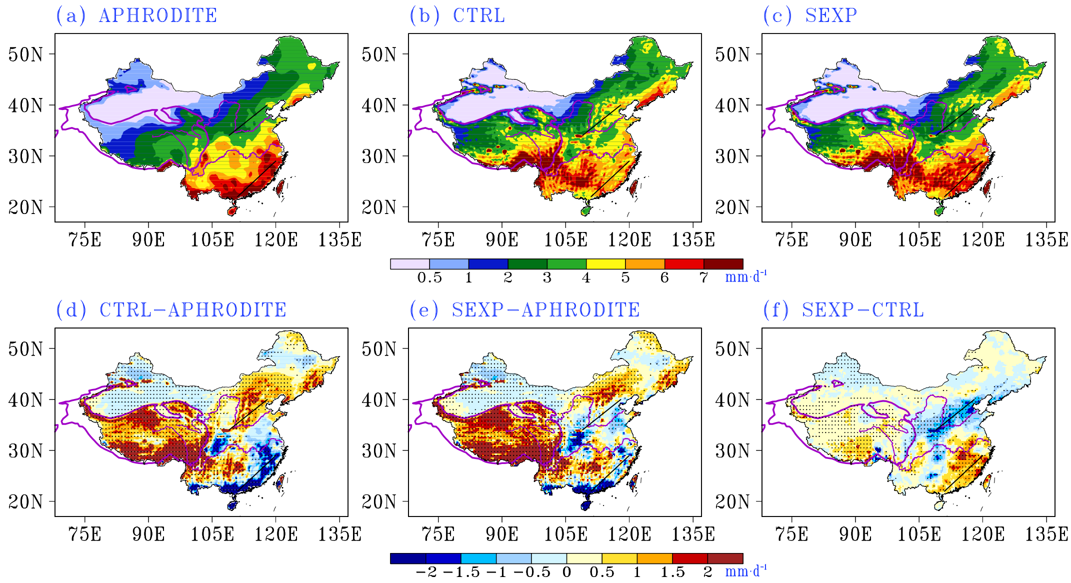

Figure 2. The precipitation from the APHRODITE data (a), the CTRL experiment (b), the SEXP experiment (c), and the precipitation differences between the CTRL experiment and the APHRODITE data (d), between the SEXP experiment and the APHRODITE data (e), and between the SEXP and CTRL experiments (f) over China averaged in summer during 2006–2015. The purple lines are the elevation contour of 3,000 m. The thin purple lines indicate the Yangtze River and the Yellow River. The black straight lines indicate centers of precipitation differences. The black dots indicate the significance above 90% of *t* test.

($R \geq 50.0$ mm·d^{-1}) precipitation. The accumulated precipitation is calculated with these four categories of precipitation. The precipitation frequency is the number of rainy days ($R \geq 0.1$ mm·d^{-1}) divided by the number of total days and the precipitation intensity is the total precipitation amount divided by the number of rainy days (Kan et al., 2015). Four sub-regions are divided for evaluation according to the propagation of summer monsoon rainfall (Ding, 1992; Ren et al., 2022): the southeastern China (Reg1, 18–26°N, 105–123°E), the mid-lower Yangtze River Basin (Reg2, 26–33°N, 107–123°E), the Huang-Huai Basin (Reg3, 33–40°N, 110–123°E), and the northeastern China (Reg4, 40–50°N, 119–130°E). The influences of the TOFD scheme on the RegCM4 performance are shown by the differences between the simulations from the SEXP and CTRL experiments. The significance of differences is determined by the Student's *t*-test (Lehmann, 1992; Student, 1908). The root mean square error (RMSE), spatial correlation coefficient (SCC), and Taylor score (TS, Taylor, 2001) are adopted to assess the simulations. Lower RMSE, higher SCC, and higher TS indicate better model performance.

3. Model Evaluation

Compared to the APHRODITE data, both the CTRL and SEXP experiments reproduce the general features of the summer precipitation over China decreasing from the southeast to the northwest (Figures 2a–2c). As shown in Figure 2d, the precipitation is underestimated (overestimated) by 2.0 mm·d^{-1} over the southeastern coast (TP) in the CTRL experiment. The SEXP experiment with the adoption of sub-grid TOFD scheme largely reduces the biases over most of eastern China (Figures 2d–2f). The sub-grid TOFD scheme enhances the ability of RegCM4 in simulating the summer precipitation over the monsoonal regions of China but slightly increases the positive precipitation bias over most of TP.

Figure 3 shows the statistics assessing the performance of simulated summer monsoon precipitation over the sub-regions of eastern China by the RegCM4 with or without the sub-grid TOFD scheme. As shown in Figure 3a, the simulated summer precipitation in the SEXP experiment is closer to the APHRODITE data than those in the CTRL experiment with the relative errors diminished by 6%, 3%, 14%, and 3% over the sub-regions. Relative to the CTRL experiment, the SEXP experiment with the sub-grid TOFD scheme can obviously improve the summer precipitation simulation over the southeastern China, the mid-lower Yangtze River Basin, and the Huang-Huai Basin with the SCC increased by 23%, 108%, and 37% (Figure 3b), meanwhile, the RMSE (TS) of the SEXP simulated summer precipitation over the southeastern China, the mid-lower Yangtze River Basin, the Huang-Huai

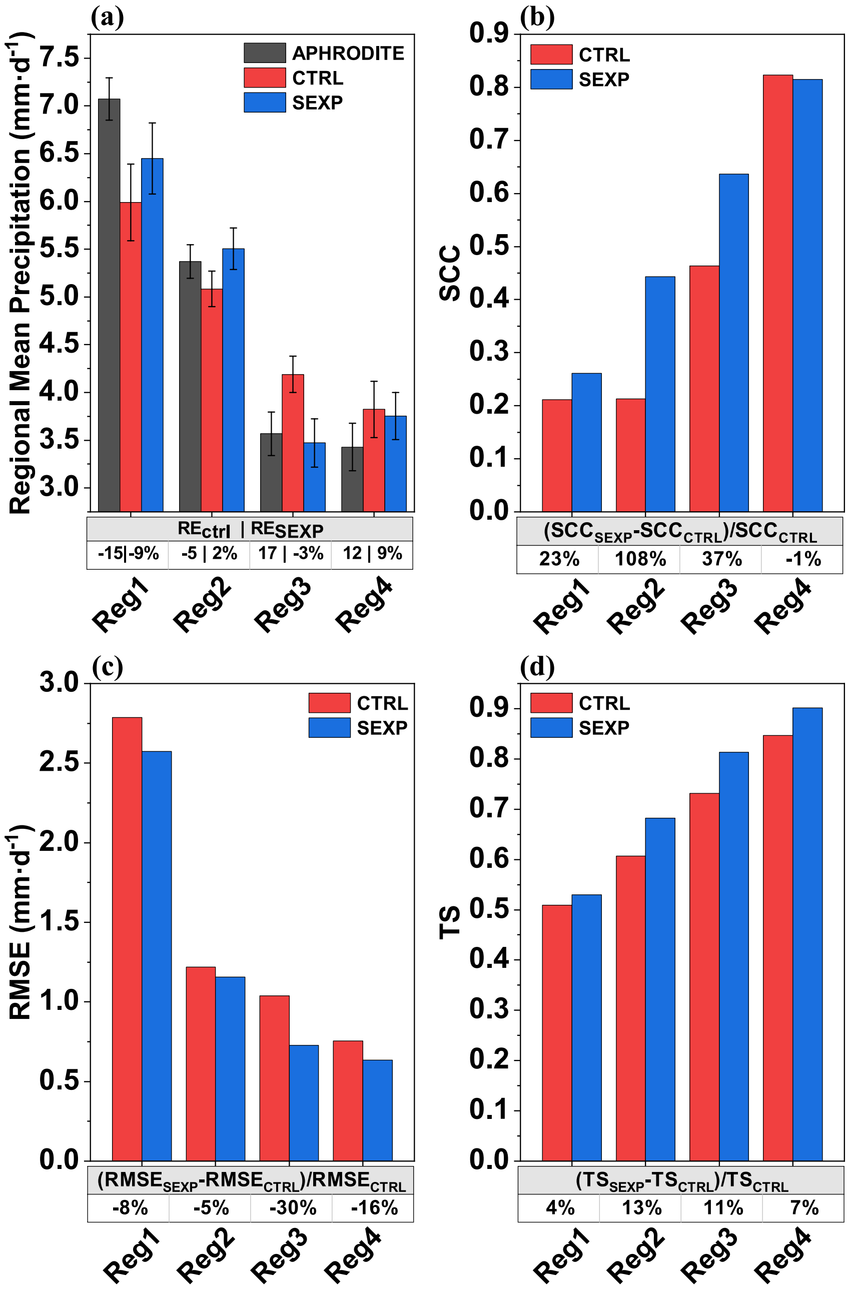

Figure 3. The average values (a), SCC (b), RMSE (c), and TS (d) of the summer precipitation over the four sub-regions averaged during 2006–2015 from the CTRL (red bar) and SEXP (blue bar) experiments against the APHRODITE data. Tables show the relative error (RE) and the relative changes of SCC, RMSE, and TS in the SEXP experiment compared to those in the CTRL experiment. The SCC all pass the significant level of 95%.

Basin, and the northeastern China against observation can be reduced (increased) by 8%, 5%, 30%, and 16% (4%, 13%, 11%, and 7%) due to the adoption of sub-grid TOFD scheme (Figures 3c and 3d). Overall, adopting the sub-grid TOFD scheme can improve the performance of RegCM4 in simulating the summer precipitation over eastern China to varying degrees.

4. Possible Physical Mechanisms

Figures 4a and 4b indicate that the differences of the simulated summer precipitation between the SEXP and CTRL experiments over the monsoonal China mainly comes from the differences of simulated precipitation

10.1029/2023JD039113

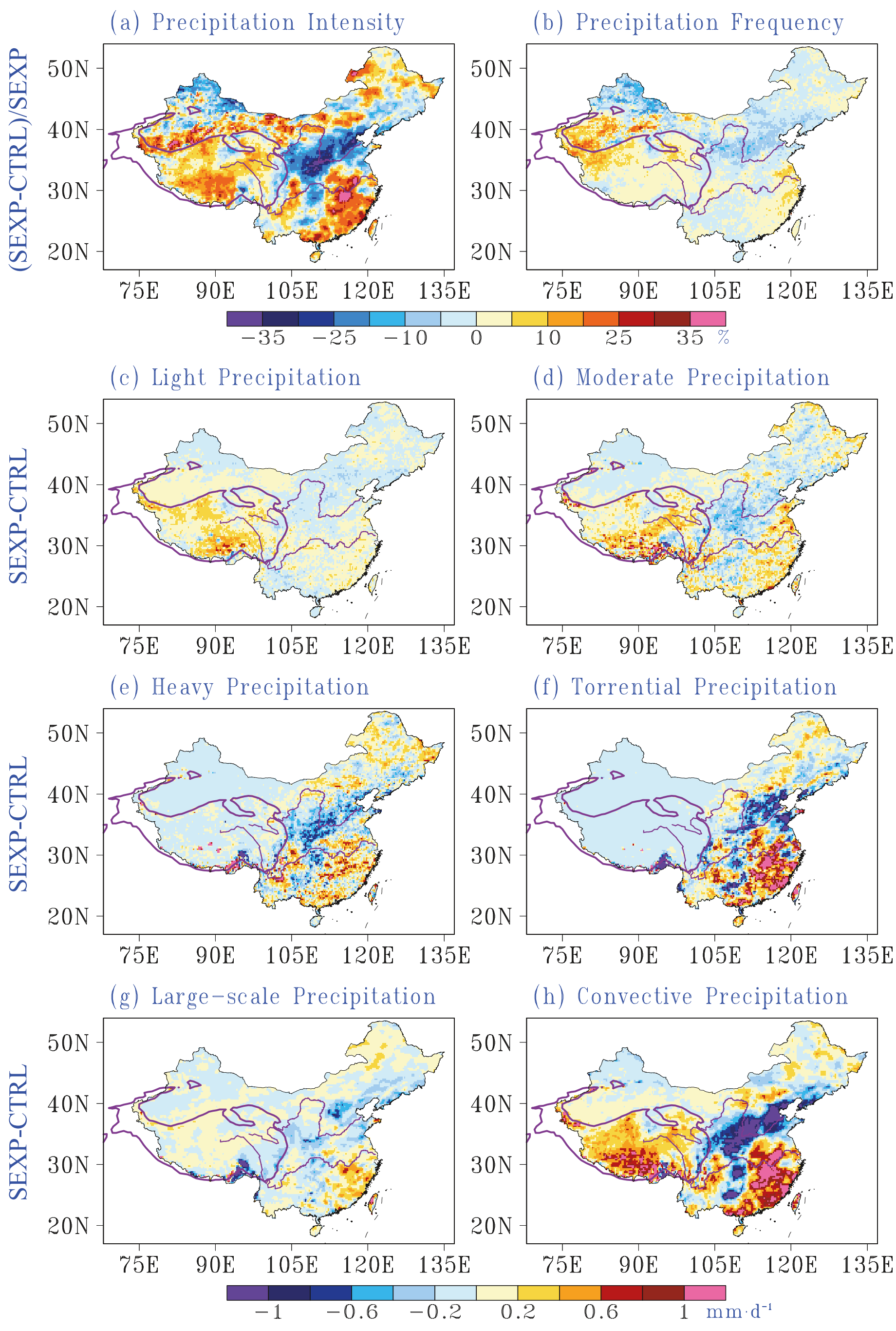

Figure 4. The differences of simulated precipitation intensity (a), precipitation frequency (b), light precipitation (c), moderate precipitation (d), heavy precipitation (e), torrential precipitation (f), large-scale precipitation (g), and convective precipitation (h) between the SEXP and CTRL experiments over China averaged in summer during 2006–2015. The purple lines are the elevation contour of 3,000 m. The thin purple lines indicate the Yangtze River and the Yellow River.

intensity rather than precipitation frequency. The differences of the light, moderate, heavy, and torrential precipitation between the SEXP and CTRL experiments share the same spatial pattern with those of the total precipitation (Figures 2f and 4c–4f). The summer precipitation over the TP primarily comes from the high frequent convective activities with the weak precipitation intensity (Ueno et al., 2001; Y. Zhao et al., 2019; Fu et al., 2020). Relative to the CTRL experiment, the SEXP experiment produced much higher positive precipitation bias over the top of the TP which is mainly attributed to the overestimated light and moderate precipitation, and reduced the heavy and torrential precipitation over the south and east edges of the TP. The improvement of simulated precipitation

AGU ADVANCING EARTH AND SPACE SCIENCES
Journal of Geophysical Research: Atmospheres
10.1029/2023JD039113

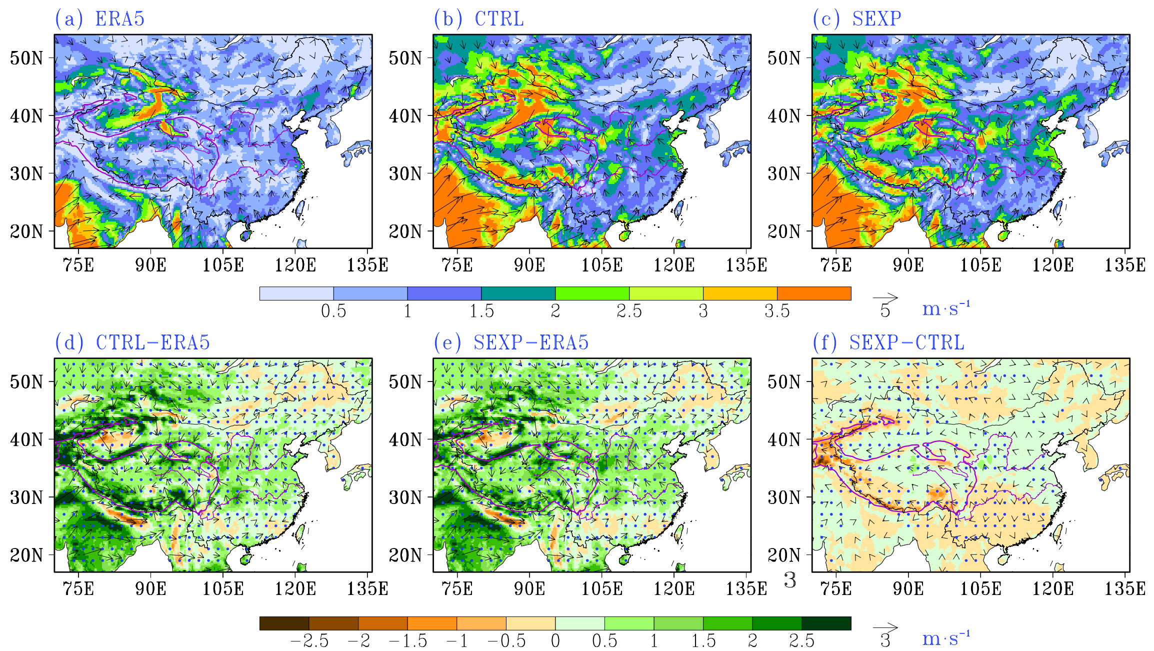

Figure 5. The wind at 10 m above the ground surface from the ERA5 data (a), the CTRL experiment (b), the SEXP experiment (c) and the differences of wind at 10 m above the ground surface between the CTRL experiment and the ERA5 data (d), between the SEXP experiment and the ERA5 data (e), and between the SEXP and CTRL experiments (f) averaged in summer during 2006–2015. The purple lines are the elevation contour of 3,000 m. The thin purple lines indicate the Yangtze River and the Yellow River. The black dots indicate the significant level above 90% of *t* test.

over eastern China in the SEXP experiment mostly comes from the improved heavy and torrential precipitation simulation. The differences of simulated convective (large-scale) precipitation between the two experiments are the major (minor) contributions to the differences of the total precipitation (Figures 4g and 4h). The simulated fractions of the convective precipitation frequency and amount in the total precipitation in the SEXP experiment are similar to those in the CTRL experiment (not shown). The improved convective or heavy to torrential precipitation benefits the improvements of summer precipitation simulation over the monsoonal region of China in the SEXP experiment by adopting the sub-grid TOFD scheme (Figures 2 and 4).

In the CTRL experiment, the RegCM4 overestimates the near surface wind over most of the land compared to the ERA5 data, and the large overestimation of the near surface wind is located over the rugged area such as the Pamir Plateau, the Tianshan Mountain, the edges of TP and hilly areas of southeastern China (Figure 5d). The errors in near surface wind simulation over the Tianshan Mountain, the Pamir Plateau, the western TP, and the southern TP can be reduced by adopting the sub-grid TOFD scheme in the SEXP experiment (Figures 5d–5f). Furthermore, the RMSE of near surface wind speed produced by the CTRL experiment over the elevated and rugged western China is much larger than that over the flat eastern China (Figure 6a) and mainly comes from the simulation of zonal wind component (Figures 6a–6c). Relative to the CTRL experiment, the SEXP experiment with the sub-grid TOFD scheme can significantly reduce the RMSE of near surface wind simulation over the Tianshan Mountain, Pamir Plateau, and southern TP (Figures 6d–6i). Overall, the sub-grid TOFD scheme can offer the RegCM4 to describe the SOD and reasonably reproduce the near surface wind field over the rugged areas.

Figures 7a–7f show that the direction of simulated TOFD acceleration in the SEXP experiment is the opposite of the direction of simulated horizontal wind velocity in the CTRL experiment at each vertical layer, which indicates that the TOFD directly slow down the local horizontal wind speed but do not affect the local horizontal wind direction over the regions with complex terrain. The TOFD primarily affects the horizontal wind directly in the planetary boundary layer (below 1,000 m in Beljaars et al., 2004). The TP has the highest elevation and most complex terrain among East Asia with the elevation rising from 3,000 to 6,000 m (Figure 1a). Therefore, the planetary boundary layer of the TP can be 4,000–7,000 m above the sea level. The pressure layers of 925, 850, 700, 600, 500, and 400 hPa are about 700, 1,500, 3,000, 4,000, 5,500, and 7,000 m above the sea level. Thus, the TOFD acceleration over the monsoonal China are mainly generated at the layers below 700 hPa while the TOFD

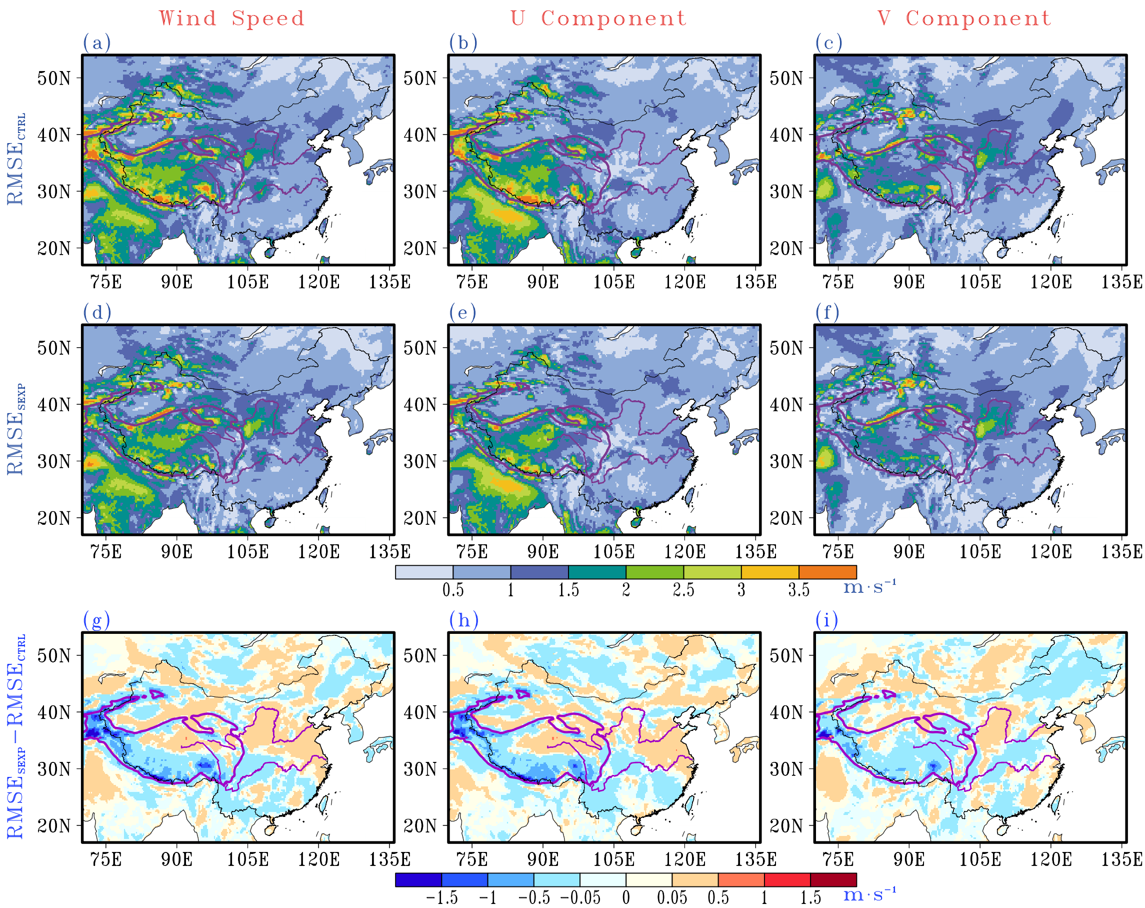

Figure 6. The RMSE of simulated wind speed at 10 m above the ground surface (a, d), zonal component (b, e), and meridional component (c, f) averaged in summer during 2006–2015 from the CTRL (a-c) and SEXP (d-f) experiments against those from the ERA5 data. The RMSE differences of simulated wind speed at 10 m above the ground surface (g), zonal component (h), and meridional component (i) between the SEXP and CTRL experiments. The purple lines are the elevation contour of 3,000 m. The thin purple lines indicate the Yangtze River and the Yellow River.

acceleration over the TP can affect the simulated horizontal wind velocity at 400 hPa (Figures 7a–7f and 8). The TOFD acceleration over the western China especially the TP is much stronger than those over the eastern China (Figure 8). In addition, Figures 7g–7l further show the differences of simulated wind at different vertical layers from 925 to 400 hPa between the SEXP and CTRL experiments. Compared to the CTRL experiment, the SEXP experiment with the sub-grid TOFD scheme makes the RegCM4 generate cyclonic (anti-cyclonic) wind differences over the southeastern (northeastern) China and the TP (northwestern China), which are the synergistic influence of the local TOFD acceleration and the wind differences propagated from the upper stream rugged areas. Because the TOFD accelerations over eastern China are below 700 hPa (Figure 8b), the wind differences in the middle troposphere over eastern China primarily comes from the propagation of the wind differences over the western region, especially over the TP. Both the cyclonic and anti-cyclonic wind differences extend from the boundary layer to the mid-troposphere (Figures 7g–7l) and lead to profound impacts on the atmospheric stability, the vertical motion, and the water vapor transport (Figures 9 and 10).

The precipitation differences between the SEXP and CTRL experiments (Figure 2f) could not be well explained alone by the differences of the convective available potential energy (CAPE), the water vapor transport, or the low-level troposphere vertical motion (Figures 9a–9c). However, the precipitation differences are totally in consistent with the differences of the middle troposphere vertical motion averaged from 600 to 400 hPa (Figures 2f and 9d). Although the water vapor transport and the CAPE are two of the determining factors for the summer monsoonal rainfall (Dong et al., 2019; Zhou & Yu, 2005), the low-level atmospheric feedback to the TOFD (Figures 9a–9c) are not the main reason for the precipitation differences over the eastern China between the SEXP and CTRL experiments in this study. The large-scale atmospheric circulation can regulate the rainfall

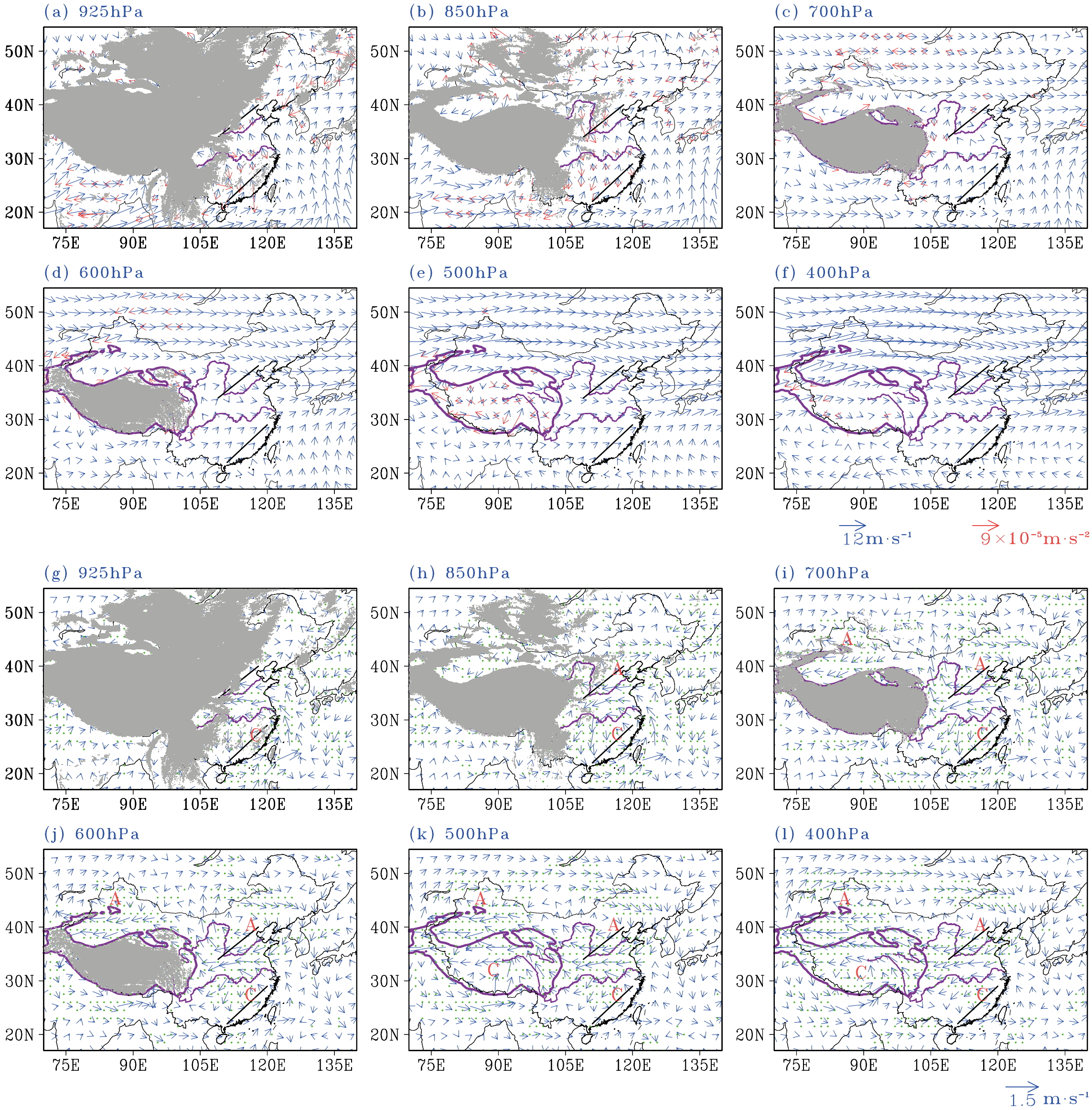

Figure 7. The simulated summer wind in the CTRL experiments (blue vector), the TOFD acceleration (red vector) in the SEXP at 925 hPa (a), 850 hPa (b), 700 hPa (c), 600 hPa (d), 500 hPa (e), and 400 hPa (f) averaged over 2006–2015. The differences of simulated summer wind between the SEXP and CTRL experiments at 925 hPa (g), 850 hPa (h), 700 hPa (i), 600 hPa (j), 500 hPa (k), and 400 hPa (l) averaged during 2006–2015. The thick purple lines are the elevation contour of 3,000 m. The thin purple lines indicate the Yangtze River and the Yellow River. The gray shade indicates the topography above the vertical layer in panels (a–d) and (g–j). The green dots indicate the significance above 90% of *t* test. The red character "C" and "A" indicate the center of cyclonic and anti-cyclonic wind differences. The black straight lines indicate the centers of precipitation differences.

in the aspects of locations and intensity (Miao et al., 2019; Zhang et al., 2008). The differences of the middle troposphere vertical motion (Figure 9d) result in the differences of the precipitation intensity (Figure 4) and thereafter precipitation amount (Figure 2).

Figures 10a,10c,10d and 10f indicate more (less) stable atmospheric stratification and weaker (stronger) ascending motion in the middle troposphere are simulated in the SEXP experiment compared to those in the CTRL experiment, leading to the negative (positive) precipitation differences in Figure 2f. Similar to Figures 9, Figure 10 also shows that the differences of the atmospheric stability, the water vapor transport, and the vertical motion in the low-level troposphere are not the essential reason for the precipitation differences between the SEXP and CTRL experiments.

In all, the sub-grid TOFD scheme provides the RegCM4 a better description of the SOD, which results in the improvements of simulated horizontal wind (Figures 5 and 6) over the regions with complex terrain (such as

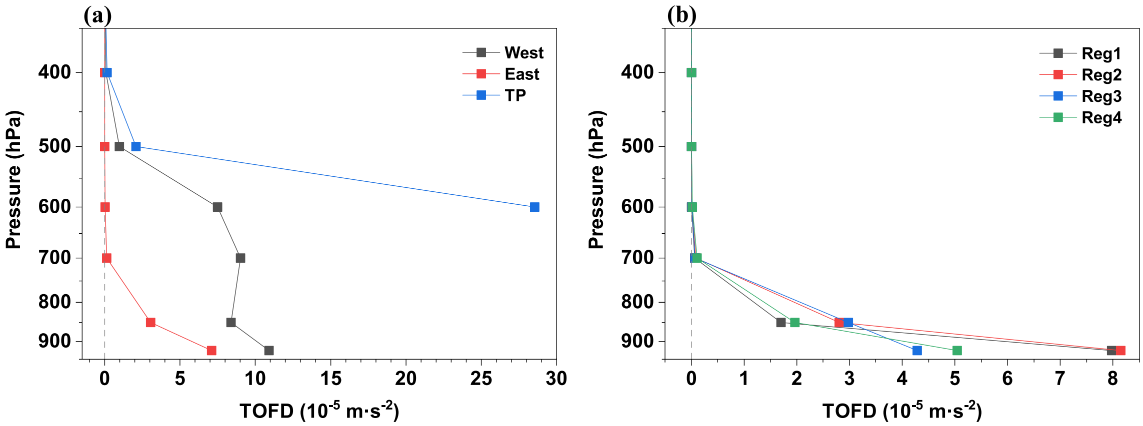

Figure 8. The profiles of the regionally averaged simulated summer TOFD acceleration over the lands of the sub-regions divided in Figure 1.

the TP). Due to the evolution and propagation of the atmospheric circulation, the TOFD not only slows down the local horizontal wind over the complex terrains but also induces horizontal wind differences over the downstream of the rugged areas (Figure 7). The TOFD over western China especially over the TP greatly contributes to the horizontal wind differences and thereafter vertical motion differences over the monsoonal China (Figures 7 and 8). The differences of the vertical motion in the middle troposphere primarily determine the precipitation differences over monsoonal China through regulating the precipitation intensity (Figures 2f, 4, 9, and 10).

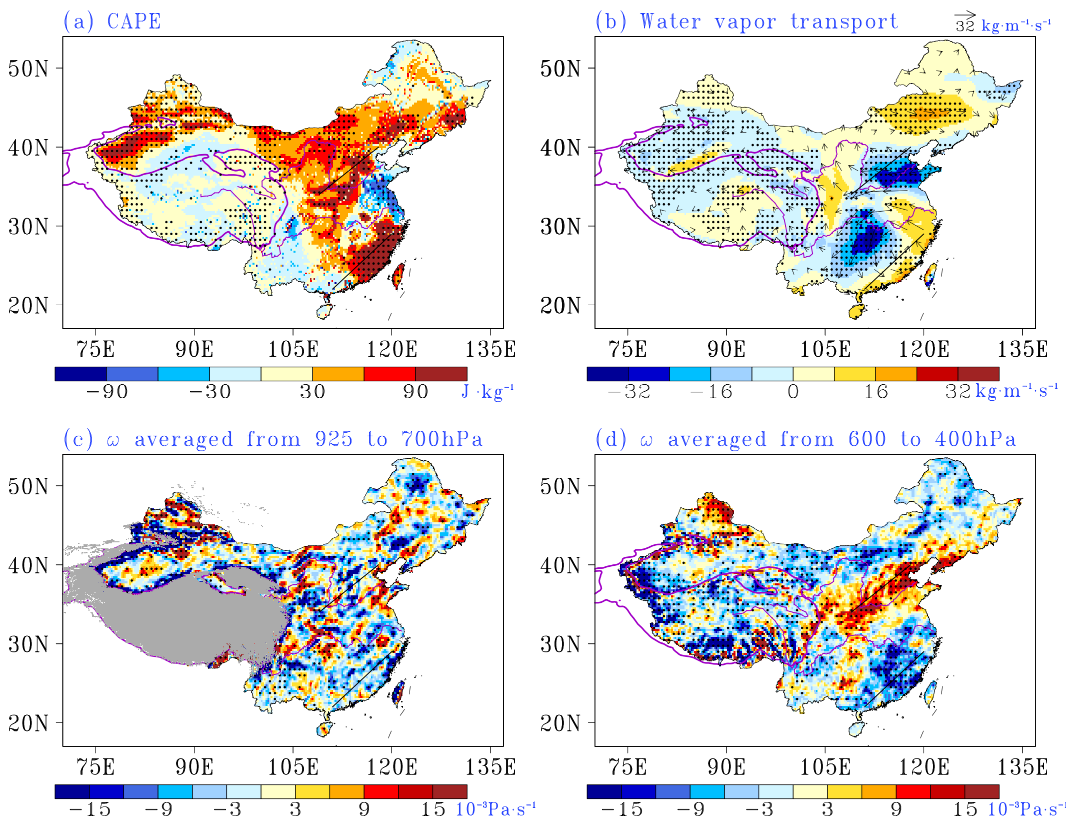

Figure 9. The differences of simulated convective available potential energy (a), the water vapor transport (integral from the surface to 100 hPa) (b), the low-level troposphere vertical speed ω averaged from 925 to 700 hPa (c), and the mid-level troposphere vertical speed ω averaged from 600 to 400 hPa (d) between the SEXP and CTRL experiments over China averaged in summer during 2006–2015. The thick purple lines are the elevation contour of 3,000 m. The thin purple lines indicate the Yangtze River and the Yellow River. The gray shade indicates the topography above the vertical layer. The green dots indicate the significance above 90% of *t* test. The black straight lines indicates centers of precipitation differences.

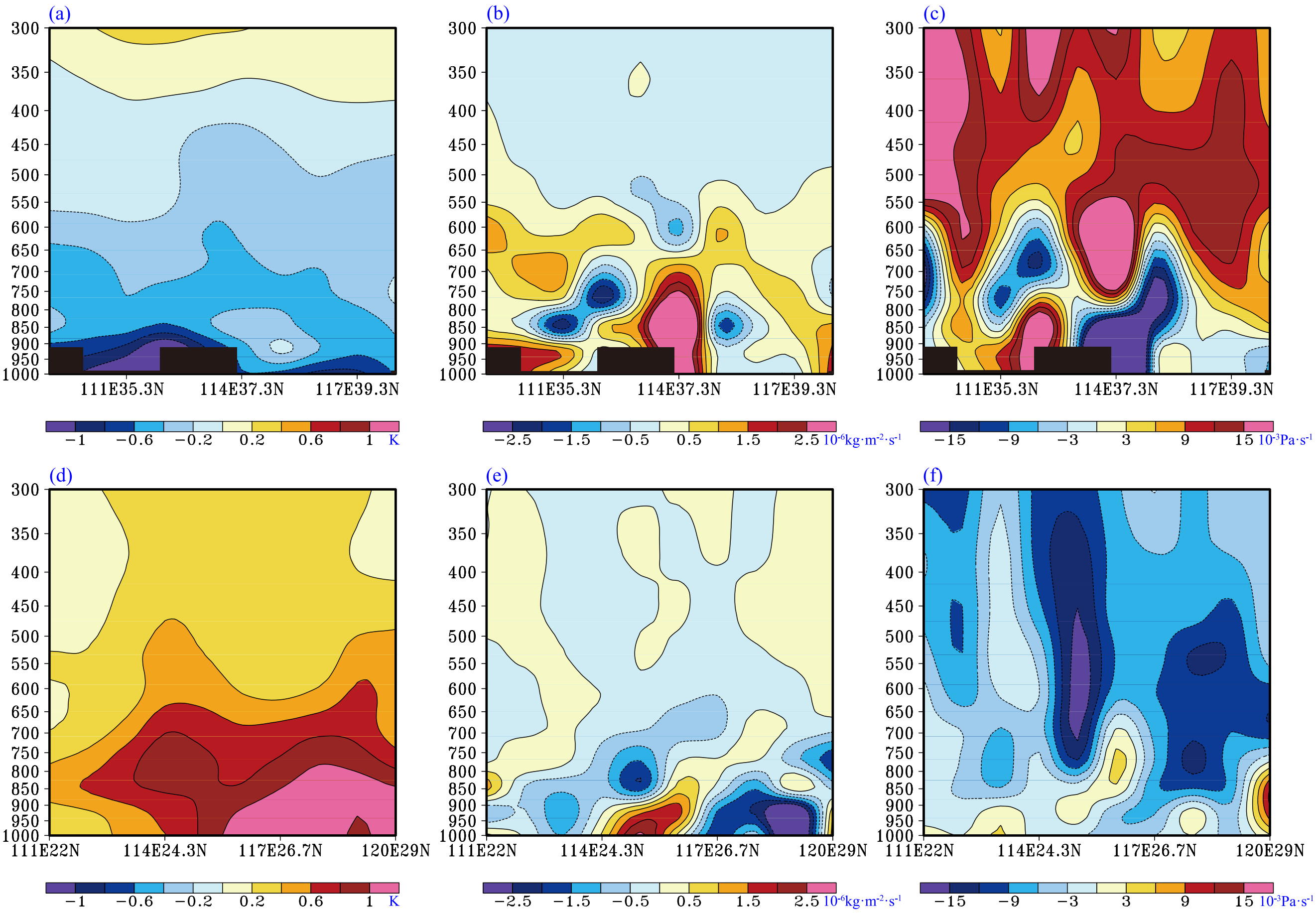

Figure 10. The cross-section of the differences of simulated potential pseudo-equivalent temperature θ_{se} (a, d), the water vapor flux divergence (b, e), and the vertical speed ω (c, f) between the SEXP and CTRL experiments over China averaged in summers of 2006–2015. Panels (a–c) and (d–f) are the cross-section in the large negative (positive) precipitation difference center shown in Figure 2f.

5. Conclusion and Discussion

Previous studies show that the micro-scale terrain has great impacts on the weather and the sub-grid TOFD scheme improves the ability of model in weather forecast. However, the importance of the sub-grid TOFD scheme is not well recognized in the climatic modeling of precipitation. In this study, the sub-grid TOFD scheme has been introduced into the RegCM4 to improve the description of SOD and its impacts on the performance of the RegCM4 in simulating the summer precipitation over China has been investigated based on two numerical experiments using the RegCM4 with or without the sub-grid TOFD scheme in ten summers of 2006–2015. The main results are listed as following:

The original RegCM4 overestimates the wind over the rugged areas due to the absent of SOD, which leads to the unrealistic simulated atmospheric circulation and thereafter precipitation. The adoption of sub-grid TOFD scheme can remarkably improves the ability of the RegCM4 in simulating summer precipitation over monsoonal region of China in the aspect of both the spatial distribution and the magnitude. Relative to those in the CTRL experiment, the SCC of summer precipitation simulated by the SEXP experiment with the adoption of sub-grid TOFD scheme over the southeastern China, the mid-lower Yangtze River Basin, and the Huang-Huai Basin can be improved by 23%, 108%, and 37%, respectively, and the RMSE (TS) of the SEXP experiment simulated summer precipitation over the southeastern China, the mid-lower Yangtze River Basin, the Huang-Huai Basin, and the northeastern China in the SEXP experiment is decreased (increased) by 8%, 5%, 30%, and 16% (4%, 13%, 11%, and 7%), respectively.

The improvements of the modeled precipitation over the monsoonal China are mainly attributed to the changes of the precipitation intensity (heavy to torrential precipitation) and convective precipitation simulation, which is resulted from the better produced atmospheric circulation due to the adoption of sub-grid TOFD scheme. The TOFD scheme improves the ability of the RegCM4 in describing the SOD and evidently reduces the biases of near surface wind simulated by the original RegCM4 over the southern TP, Tianshan Mountain, Pamir Plateau, and Yungui Plateau. Compared to the CTRL experiment, the SEXP experiment adopting the TOFD scheme generates cyclonic (anti-cyclonic) wind differences over the southeastern (northeastern) China from the boundary layer to the mid-troposphere. The wind differences over the monsoonal China are attributed to the wind differences propagated from the rugged upstream area (TP) and the local TOFD acceleration. Then the vertical motion, the atmospheric stability, and the water vapor transport adapt to the wind differences. The vertical motion differences in the middle troposphere determine the precipitation differences and the negative (positive) precipitation differences are in consistent with the downward (upward) vertical motion differences.

Previous studies have shown that the East Asia Summer Monsoon (EASM) is mainly controlled by the thermal effects of the TP (Duan & Wu, 2005; Wu et al., 2007), which excite the Rossby wave and greatly affect the downstream precipitation (B. Wang et al., 2008; Y. Wang et al., 2011). The results of this study are in accordance with the recent studies (Son et al., 2019, 2020) which claim that mechanical forcing also plays an important role in the formation and development of precipitation during the EASM. Meanwhile, the adoption of the sub-grid TOFD scheme increases the wet bias over the TP with more convective and light precipitation. Our recent study shows that the parameterization of 3D sub-grid terrain solar radiation effects (3DSTSRE) reduces the wet biases over the TP in the RegCM4 (C. Gu et al., 2022). Thus, the collaborative influences and relative importance of the sub-grid TOFD scheme and 3DSTSRE scheme on the numerical modeling should be addressed in the future work.

Although this study shows the necessity of sub-grid TOFD scheme for the climate modeling, we have to admit this study has its disadvantages. It only provides an elementary evaluation of the sub-grid TOFD scheme on the performance of the RegCM4 due to the limitation of discontinuous simulations in 10 summers over East Asia by the hydro-static RegCM4 with moderate resolution. The readers must check the model performance if the TOFD scheme is applied in the RegCM4 with the different configurations of domain, physical schemes, forcing data, dynamic cores, regions, and seasons. The relative importance of sub-grid TOFD due to the terrain over the upstream areas and the local areas on the monsoonal precipitation are not revealed quantitatively, which is investigated now and will be reported in near future. We also preliminary find that the impacts of the TOFD scheme on the ability of the RegCM4 in simulating the summer precipitation is more evident during the flood years than during the drought years in eastern China. The impacts of the sub-grid TOFD scheme on the climate modeling over China under different climatic backgrounds should also be investigated with the long-term simulations. In addition, more detailed investigations about the RegCM4/RegCM5 with the sub-grid TOFD scheme should be conducted based on the non-hydrostatic simulations with high resolution across the world.

Data Availability Statement

Data—The data used in this study are the daily 0.25° × 0.25° gridded precipitation provided by Asian Precipitation Highly-Resolved Observational Data Integration Towards Evaluation (APHRODITE, 2012), the hourly 0.25° × 0.25° ERA5 atmospheric reanalyses (ECMWF, 2020), the 30″ × 30″ Global Multi-resolution Terrain Elevation Data (GMTED, Danielson & Gesch, 2011), the weekly 1.0° × 1.0° NOAA Optimum Interpolation Sea Surface Temperature (OISST, NOAA, 2002), the 0.25° × 0.25° European Space Agency (ESA) Climate Change Initiative (CCI) Essential Climate Variable (ECV) Surface Soil Moisture Combined Product (Dorigo et al., 2021), the hourly 1.5° × 1.5° ERA-Interim reanalysis (ECMWF, 2011). Software—The RegCM4 with the TOFD scheme (Gu et al., 2023) and the original RegCM4 without the TOFD scheme (ICTP, 2016).

Acknowledgments

This study is supported by the National Natural Science Foundation of China under Grant 42375157, the National Natural Science Foundation of China under Grant 41975081, the Postgraduate Research and Practice Innovation Program of Jiangsu Province (No. 124 in 2023), the CAS "Light of West China" Program (E129030101), Open Research Fund Program of Plateau Atmosphere and Environment Key Laboratory of Sichuan Province (PAEKL-2023-K01), the Research Funds for the Frontiers Science Center for Critical Earth Material Cycling Nanjing University, the Fundamental Research Funds for the Central Universities (020914380103), the Jiangsu University "Blue Project" outstanding young teachers training object, and the Jiangsu Collaborative Innovation Center for Climate Change. We appreciate ICTP for providing the RegCM4 (https://github.com/ictp-esp/RegCM). We are grateful to ECMWF, APHRODITE, USGS, ESA, and NOAA for allowing us to use their data sets. We show our warm appreciation and deepest respect to the three anonymous reviewers for their constructive suggestions to greatly improve the manuscript.

References

Alapaty, K., Herwehe, J. A., Otte, T. L., Nolte, C. G., Bullock, O. R., Mallard, M. S., et al. (2012). Introducing subgrid-scale cloud feedbacks to radiation for regional meteorological and climate modeling. *Geophysical Research Letters*, *39*(24), L24809. https://doi.org/10.1029/2012GL054031

Anders, A. M., Roe, G. H., Montgomery, D. R., & Hallet, B. (2008). Influence of precipitation phase on the form of mountain ranges. *Geology*, *36*(6), 479–482. https://doi.org/10.1130/g24821a.1

APHRODITE. (2012). A long-term daily gridded precipitation dataset for Asia based on a dense network of rain gauges [Datasets]. APHRODITE. Retrieved from http://aphrodite.st.hirosaki-u.ac.jp/download/

Athanassiadou, M. (2003). Wave and form drag: Their relation in the linear gravity wave regime. *Tellus A: Dynamic Meteorology and Oceanography*, *55*(2), 173–180. https://doi.org/10.3402/tellusa.v55i2.12090

Bao, J., Feng, J., & Wang, Y. (2015). Dynamical downscaling simulation and future projection of precipitation over China. *Journal of Geophysical Research: Atmospheres*, *120*(16), 8227–8243. https://doi.org/10.1002/2015JD023275

Barry, R. G. (2008). *Mountain weather and climate* (3rd ed.). Cambridge University Press. https://doi.org/10.1017/CBO9780511754753

Becker, E., & Vadas, S. L. (2018). Secondary gravity waves in the winter mesosphere: Results from a high-resolution global circulation model. *Journal of Geophysical Research: Atmospheres*, *123*(5), 2605–2627. https://doi.org/10.1002/2017JD027460

Belcher, S. E., & Wood, N. (1996). Form and wave drag due to stably stratified turbulent flow over low ridges. *Quarterly Journal of the Royal Meteorological Society*, *122*(532), 863–902. https://doi.org/10.1002/qj.49712253205

Beljaars, A. C. M., Brown, A. R., & Wood, N. (2004). A new parametrization of turbulent orographic form drag. *Quarterly Journal of the Royal Meteorological Society*, *130*(599), 1327–1347. https://doi.org/10.1256/qj.03.73

Boroneant, C., Plaut, G., Giorgi, F., & Bi, X. (2006). Extreme precipitation over the Maritime Alps and associated weather regimes simulated by a regional climate model: Present-day and future climate scenarios. *Theoretical and Applied Climatology*, *86*(1), 81–99. https://doi.org/10.1007/s00704-005-0211-7

Cannon, F., Carvalho, L. M. V., Jones, C., Norris, J., Bookhagen, B., & Kiladis, G. N. (2017). Effects of topographic smoothing on the simulation of winter precipitation in High Mountain Asia. *Journal of Geophysical Research: Atmospheres*, *122*(3), 1456–1474. https://doi.org/10.1002/2016JD026038

Charney, J. G., & Eliassen, A. (1949). A numerical method for predicting the perturbations of the middle latitude westerlies. *Tellus*, *1*(2), 38–54. https://doi.org/10.3402/tellusa.v1i2.8500

Chen, H., Zhou, T., Neale, R. B., Wu, X., & Zhang, G. (2010). Performance of the new NCAR CAM3. 5 in East Asian summer monsoon simulations: Sensitivity to modifications of the convection scheme. *Journal of Climate*, *23*(13), 3657–3675. https://doi.org/10.1175/2010JCLI3022.1

Chen, J., Yin, Y., Chen, Q., Ding, H., & Xiao, H. (2014). Effect of convection schemes on the simulation of monsoon climates: A sensitivity study using RegCM4. *Climate Research*, *60*(2), 147–162. https://doi.org/10.3354/CR01229

Chen, S., Hamdi, R., Ochege, F. U., Du, H., Chen, X., Yang, W., & Zhang, C. (2019). Added value of a dynamical downscaling approach for simulating precipitation and temperature over Tianshan Mountains Area, Central Asia. *Journal of Geophysical Research: Atmospheres*, *124*(21), 11051–11069. https://doi.org/10.1029/2019JD031016

Choi, H., & Hong, S. (2015). An updated subgrid orographic parameterization for global atmospheric forecast models. *Journal of Geophysical Research-Atmospheres*, *120*(24), 12445–12457. https://doi.org/10.1002/2015jd024230

Coppola, E., Stocchi, P., Pichelli, E., Torres Alavez, J. A., Glazer, R., Giuliani, G., et al. (2021). Non-hydrostatic RegCM4 (RegCM4-NH): Model description and case studies over multiple domains. *Geoscientific Model Development*, *14*(12), 7705–7723. https://doi.org/10.5194/gmd-14-7705-2021

Danielson, J. J., & Gesch, D. B. (2011). Global multi-resolution terrain elevation data 2010 (GMTED2010) [Datasets]. USGS. https://doi.org/10.3133/ofr20111073

Davis, C. A. (1997). The modification of baroclinic waves by the Rocky Mountains. *Journal of the Atmospheric Sciences*, *54*(7), 848–868. https://doi.org/10.1175/1520-0469(1997)054<0848:Tmobwb>2.0.Co;2

Dee, D. P., Uppala, S. M., Simmons, A. J., Berrisford, P., Poli, P., Kobayashi, S., et al. (2011). The ERA-Interim reanalysis: Configuration and performance of the data assimilation system. *Quarterly Journal of the Royal Meteorological Society*, *137*(656), 553–597. https://doi.org/10.1002/qj.828

Dickinson, R. E., Errico, R. M., Giorgi, F., & Bates, G. T. (1989). A regional climate model for the western United States. *Climatic Change*, *15*(3), 383–422. https://doi.org/10.1007/BF00240465

Ding, Y. (1992). Summer monsoon rainfalls in China. *Journal of the Meteorological Society of Japan. Ser. II*, *70*(1B), 373–396. https://doi.org/10.2151/jmsj1965.70.1B_373

Dong, W., Lin, Y., Wright, J. S., Xie, Y., Yin, X., & Guo, J. (2019). Precipitable water and CAPE dependence of rainfall intensities in China. *Climate Dynamics*, *52*(5), 3357–3368. https://doi.org/10.1007/s00382-018-4327-8

Dorigo, W., Preimesberger, W., Moesinger, L., Pasik, A., Scanlon, T., Hahn, S., et al. (2021). ESA soil moisture climate change initiative (Soil_Moisture_cci): COMBINED product. Version 06.1 [Dataset]. NERC EDS Centre for Environmental Data Analysis. Retrieved from https://catalogue.ceda.ac.uk/uuid/43d73291472444e6b9c2d2420dbad7d6

Duan, A., & Wu, G. (2005). Role of the Tibetan Plateau thermal forcing in the summer climate patterns over subtropical Asia. *Climate Dynamics*, *24*(7–8), 793–807. https://doi.org/10.1007/s00382-004-0488-8

ECMWF. (2011). The ECMWF reanalysis-interim (ERA-Interim) [Dataset]. ECMWF. Retrieved from https://www.ecmwf.int/en/forecasts/dataset/ecmwf-reanalysis-interim

ECMWF. (2020). The ECMWF reanalysis version 5 (ERA5) [Dataset]. ECMWF. Retrieved from https://www.ecmwf.int/en/forecasts/dataset/ecmwf-reanalysis-v5

Elvidge, A. D., Sandu, I., Wedi, N., Vosper, S. B., Zadra, A., Boussetta, S., et al. (2019). Uncertainty in the representation of orography in weather and climate models and implications for parameterized drag. *Journal of Advances in Modeling Earth Systems*, *11*(8), 2567–2585. https://doi.org/10.1029/2019ms001661

Feng, L., & Zhou, T. (2012). Water vapor transport for summer precipitation over the Tibetan Plateau: Multidata set analysis. *Journal of Geophysical Research*, *117*(D20), D20114. https://doi.org/10.1029/2011jd017012

Fiedler, F., & Panofsky, H. A. (1972). The geostrophic drag coefficient and the 'effective' roughness length. *Quarterly Journal of the Royal Meteorological Society*, *98*(415), 213–220. https://doi.org/10.1002/qj.49709841519

Fu, Y., Ma, Y., Zhong, L., Yang, Y., Guo, X., Wang, C., et al. (2020). Land-surface processes and summer-cloud-precipitation characteristics in the Tibetan Plateau and their effects on downstream weather: A review and perspective. *National Science Review*, *7*(3), 500–515. https://doi.org/10.1093/nsr/nwz226

Gao, X., & Giorgi, F. (2017). Use of the RegCM system over East Asia: Review and perspectives. *Engineering*, *3*(5), 766–772. https://doi.org/10.1016/J.ENG.2017.05.019

Gao, X., Shi, Y., & Giorgi, F. (2011). A high resolution simulation of climate change over China. *Science China Earth Sciences*, *54*(3), 462–472. https://doi.org/10.1007/s11430-010-4035-7

Gao, X., Shi, Y., Han, Z., Wang, M., Wu, J., Zhang, D., et al. (2017). Performance of RegCM4 over major river basins in China. *Advances in Atmospheric Sciences*, *34*(4), 441–455. https://doi.org/10.1007/s00376-016-6179-7

Gao, X., Wang, M., & Giorgi, F. (2013). Climate change over China in the 21st century as simulated by BCC_CSM1.1-RegCM4.0. *Atmospheric and Oceanic Science Letters*, *6*(5), 381–386. https://doi.org/10.3878/j.issn.1674-2834.13.0029

Gao, X., Xu, Y., Zhao, Z. C., Pal, J., & Giorgi, F. (2006). On the role of resolution and topography in the simulation of East Asia precipitation. *Theoretical and Applied Climatology*, *86*(1–4), 173–185. https://doi.org/10.1007/s00704-005-0214-4

Garvert, M. F., Smull, B., & Mass, C. (2007). Multiscale mountain waves influencing a major orographic precipitation event. *Journal of the Atmospheric Sciences*, *64*(3), 711–737. https://doi.org/10.1175/jas3876.1

Ge, J., Qiu, B., Chu, B., Li, D., Jiang, L., Zhou, W., et al. (2021). Evaluation of coupled regional climate models in representing the local biophysical effects of afforestation over continental China. *Journal of Climate*, *34*(24), 9879–9898. https://doi.org/10.1175/jcli-d-21-0462.1

Giorgi, F. (1990). Simulation of regional climate using a limited area model nested in a general circulation model. *Journal of Climate*, *3*(9), 941–963. https://doi.org/10.1175/1520-0442(1990)003<0941:Sorcua>2.0.Co;2

Giorgi, F., & Bates, G. T. (1989). The climatological skill of a regional model over complex terrain. *Monthly Weather Review*, *117*(11), 2325–2347. https://doi.org/10.1175/1520-0493(1989)117<2325:Tcsoar>2.0.Co;2

Giorgi, F., Coppola, E., Giuliani, G., Ciarlo, J. M., Pichelli, E., Nogherotto, R., et al. (2023). The fifth generation regional climate modeling system, RegCM5: Description and illustrative examples at parameterized convection and convection-permitting resolutions. *Journal of Geophysical Research: Atmospheres*, *128*(6), e2022JD038199. https://doi.org/10.1029/2022JD038199

Giorgi, F., Coppola, E., Solmon, F., Mariotti, L., Sylla, M., Bi, X., et al. (2012). RegCM4: Model description and preliminary tests over multiple CORDEX domains. *Climate Research*, *52*, 7–29. https://doi.org/10.3354/cr01018

Giorgi, F., Marinucci, M. R., & Bates, G. T. (1993). Development of a second-generation regional climate model (RegCM2). Part I: Boundary-layer and radiative transfer processes. *Monthly Weather Review*, *121*(10), 2794–2813. https://doi.org/10.1175/1520-0493(1993)121<2794:Doasgr>2.0.Co;2

Grell, G. A., Dudhia, J., & Stauffer, D. R. (1994). Description of the fifth generation Penn State/NCAR mesoscale model (MM5). *Tech. Rep. TN-398+STR, NCAR.*

Gu, C., Huang, A., Li, X., Yang, B., Zhou, X., & Wu, Y. (2023). The source codes of sub-grid turbulent orographic form drag parameterization scheme suitable for the regional climate model version 4.5.0 (RegCM4) [Software]. Zenodo. https://doi.org/10.5281/zenodo.8077329

Gu, C., Huang, A., Zhang, Y., Yang, B., Cai, S., Xu, X., et al. (2022). The wet bias of RegCM4 over tibet plateau in summer reduced by adopting the 3D sub-grid terrain solar radiative effect parameterization scheme. *Journal of Geophysical Research: Atmospheres*, *127*(21), e2022JD037434. https://doi.org/10.1029/2022JD037434

Hersbach, H., Bell, B., Berrisford, P., Hirahara, S., Horányi, A., Muñoz-Sabater, J., et al. (2020). The ERA5 global reanalysis. *Quarterly Journal of the Royal Meteorological Society*, *146*(730), 1999–2049. https://doi.org/10.1002/qj.3803

Holtslag, A. A. M., De Bruijn, E. I. F., & Pan, H. L. (1990). A high resolution air mass transformation model for short-range weather forecasting. *Monthly Weather Review*, *118*(8), 1561–1575. https://doi.org/10.1175/1520-0493(1990)118<1561:ahramt>2.0.co;2;2

Huang, D., & Gao, S. (2018). Impact of different reanalysis data on WRF dynamical downscaling over China. *Atmospheric Research*, *200*, 25–35. https://doi.org/10.1016/j.atmosres.2017.09.017

ICTP. (2016). The regional climate model version 4.5.0 (RegCM4) [Software]. Zenodo. https://doi.org/10.5281/zenodo.8077329

Jiang, D., Hu, D., Tian, Z., & Lang, X. (2020). Differences between CMIP6 and CMIP5 models in simulating climate over China and the East Asian monsoon. *Advances in Atmospheric Sciences*, *37*(10), 1102–1118. https://doi.org/10.1007/s00376-020-2034-y

Jiang, D., Tian, Z., & Lang, X. (2016). Reliability of climate models for China through the IPCC third to fifth assessment reports. *International Journal of Climatology*, *36*(3), 1114–1133. https://doi.org/10.1002/joc.4406

Kain, J. S., & Fritsch, J. M. (1990). A one-dimensional entraining/detraining plume model and its application in convective parameterization. *Journal of the Atmospheric Sciences*, *47*(23), 2784–2802. https://doi.org/10.1175/1520-0469(1990)047<2784:aodepm>2.0.co;2

Kan, M. Y., Huang, A. N., Zhao, Y., Zhou, Y., Yang, B., & Wu, H. (2015). Evaluation of the summer precipitation over China simulated by BCC_CSM model with different horizontal resolutions during the recent half century. *Journal of Geophysical Research: Atmospheres*, *120*(10), 4657–4670. https://doi.org/10.1002/2015JD023131

Kendon, E. J., Ban, N., Roberts, N. M., Fowler, H. J., Roberts, M. J., Chan, S. C., et al. (2017). Do convection-permitting regional climate models improve projections of future precipitation change? *Bulletin of the American Meteorological Society*, *98*(1), 79–93. https://doi.org/10.1175/bams-d-15-0004.1

Kiehl, J. T., Hack, J. J., Bonan, G. B., Boville, B. A., Williamson, D. L., & Rasch, P. J. (1998). The national center for atmospheric research community climate model: CCM3. *Journal of Climate*, *11*(6), 1131–1149. https://doi.org/10.1175/1520-0442(1998)011<1131:tncfar>2.0.co;2;2

Kim, Y. J., & Doyle, J. D. (2005). Extension of an orographic-drag parametrization scheme to incorporate orographic anisotropy and flow blocking. *Quarterly Journal of the Royal Meteorological Society*, *131*(609), 1893–1921. https://doi.org/10.1256/qj.04.160

Koo, M.-S., Choi, H.-J., & Han, J.-Y. (2018). A parameterization of turbulent-scale and mesoscale orographic drag in a global atmospheric model. *Journal of Geophysical Research: Atmospheres*, *123*(16), 8400–8417. https://doi.org/10.1029/2017JD028176

Kusunoki, S. (2018). Is the global atmospheric model MRI-AGCM3.2 better than the CMIP5 atmospheric models in simulating precipitation over East Asia? *Climate Dynamics*, *51*(11), 4489–4510. https://doi.org/10.1007/s00382-016-3335-9

Lee, J., Shin, H., Hong, S., Jiménez, P. A., Dudhia, J., & Hong, J. (2015). Impacts of subgrid-scale orography parameterization on simulated surface layer wind and monsoonal precipitation in the high-resolution WRF model. *Journal of Geophysical Research: Atmospheres*, *120*(2), 644–653. https://doi.org/10.1002/2014JD022747

Lehmann, E. L. (1992). Introduction to Student (1908) the probable error of a mean. In S. Kotz & N. L. Johnson (Eds.), *Breakthroughs in statistics: Methodology and distribution* (pp. 29–32). Springer New York. https://doi.org/10.1007/978-1-4612-4380-9_3

Li, G., Chen, H., Xu, M., Zhao, C., Zhong, L., Li, R., et al. (2022). Impacts of topographic complexity on modeling moisture transport and precipitation over the Tibetan plateau in summer. *Advances in Atmospheric Sciences*, *39*(7), 1151–1166. https://doi.org/10.1007/s00376-022-1409-7

Liang, X., Sun, C., Zheng, X., Dai, Y., Xu, M., Choi, H., et al. (2019). CWRF performance at downscaling China climate characteristics. *Climate Dynamics*, *52*(3), 2159–2184. https://doi.org/10.1007/s00382-018-4257-5

Liang, X., Xu, M., Yuan, X., Ling, T., Choi, H., Zhang, F., et al. (2012). Regional climate-weather research and forecasting model. *Bulletin of the American Meteorological Society*, *93*(9), 1363–1387. https://doi.org/10.1175/bams-d-11-00180.1

Lin, C., Chen, D., Yang, K., & Ou, T. (2018). Impact of model resolution on simulating the water vapor transport through the central Himalayas: Implication for models' wet bias over the Tibetan Plateau. *Climate Dynamics*, *51*(9–10), 3195–3207. https://doi.org/10.1007/s00382-018-4074-x

Lott, F., & Miller, M. J. (1997). A new subgrid-scale orographic drag parametrization: Its formulation and testing. *Quarterly Journal of the Royal Meteorological Society*, *123*(537), 101–127. https://doi.org/10.1256/smsqj.53703

Lu, C., Huang, G., & Wang, X. (2019). Projected changes in temperature, precipitation, and their extremes over China through the RegCM. *Climate Dynamics*, *53*(9), 5859–5880. https://doi.org/10.1007/s00382-019-04899-7

Ma, J., Wang, H., & Fan, K. (2015). Dynamic downscaling of summer precipitation prediction over China in 1998 using WRF and CCSM4. *Advances in Atmospheric Sciences*, *32*(5), 577–584. https://doi.org/10.1007/s00376-014-4143-y

McFarlane, N., Girard, C., & Shantz, D. W. (1986). Reduction of systematic errors in NWP and general circulation models by parameterized gravity wave drag. *Journal of the Meteorological Society of Japan. Ser. II*, *64A*(0), 713–728. https://doi.org/10.2151/jmsj1965.64A.0_713

McHall, Y. L. (1991). Planetary stationary waves in the atmosphere Part I: Orographic stationary waves. *Advances in Atmospheric Sciences*, *8*(2), 211–224. https://doi.org/10.1007/BF02658095

Miao, C., Duan, Q., Sun, Q., Lei, X., & Li, H. (2019). Non-uniform changes in different categories of precipitation intensity across China and the associated large-scale circulations. *Environmental Research Letters*, *14*(2), 025004. https://doi.org/10.1088/1748-9326/aaf306

Nguyen-Xuan, T., Lam, S. L., Giorgi, F., Coppola, E., Giuliani, G., Gao, X., & Im, E. S. (2022). Evaluation of the performance of the non-hydrostatic RegCM4 (RegCM4-NH) over southeastern China. *Climate Dynamics*, *58*(5), 1419–1437. https://doi.org/10.1007/s00382-021-05969-5

Niu, X., Tang, J., Chen, D., Wang, S., Ou, T., & Fu, C. (2021). The performance of CORDEX-EA-II simulations in simulating seasonal temperature and elevation-dependent warming over the Tibetan Plateau. *Climate Dynamics*, *57*(3), 1135–1153. https://doi.org/10.1007/s00382-021-05760-6

NOAA. (2002). The weekly NOAA optimum interpolation sea surface temperature (OISST) [Dataset]. National Oceanic and Atmospheric Administration. Retrieved from https://psl.noaa.gov/data/gridded/data.noaa.oisst.v2.html

Oleson, K. W., Lawrence, D. M., Bonan, G. B., Drewniak, B., Huang, M., Koven, C. D., et al. (2013). *Technical description of version 4.5 of the community land model (CLM)*. National Center for Atmospheric Research. NCAR technical note NCAR/TN-503 + STR.

Pal, J. S., Giorgi, F., Bi, X., Elguindi, N., Solmon, F., Gao, X., et al. (2007). Regional climate modeling for the developing world: The ICTP RegCM3 and RegCNET. *Bulletin of the American Meteorological Society*, *88*(9), 1395–1410. https://doi.org/10.1175/bams-88-9-1395

Pal, J. S., Small, E. E., & Eltahir, E. A. B. (2000). Simulation of regional-scale water and energy budgets: Representation of subgrid cloud and precipitation processes within RegCM. *Journal of Geophysical Research*, *105*(D24), 29579–29594. https://doi.org/10.1029/2000JD900415

Pan, X., Zhang, L., & Huang, C. (2020). Future climate projection in northwest China with RegCM4.6. *Earth and Space Science*, *7*(2). https://doi.org/10.1029/2019EA000819

Prein, A. F., Langhans, W., Fosser, G., Ferrone, A., Ban, N., Goergen, K., et al. (2015). A review on regional convection-permitting climate modeling: Demonstrations, prospects, and challenges. *Reviews of Geophysics*, *53*(2), 323–361. https://doi.org/10.1002/2014RG000475

Qian, W., Fu, J., & Yan, Z. (2007). Decrease of light rain events in summer associated with a warming environment in China during 1961–2005. *Geophysical Research Letters*, *34*(11), L11705. https://doi.org/10.1029/2007GL029631

Ren, Q., Liu, F., Wang, B., Yang, S., Wang, H., & Dong, W. (2022). Origins of the intraseasonal variability of East Asian summer precipitation. *Geophysical Research Letters*, *49*(4), e2021GL096574. https://doi.org/10.1029/2021GL096574

Reynolds, R. W., Rayner, N. A., Smith, T. M., Stokes, D. C., & Wang, W. (2002). An improved in situ and satellite SST analysis for climate. *Journal of Climate*, *15*(13), 1609–1625. https://doi.org/10.1175/1520-0442(2002)015<1609:aiisas>2.0.co;2;2

Sawadogo, W., Reboita, M. S., Faye, A., da Rocha, R. P., Odoulami, R. C., Olusegun, C. F., et al. (2021). Current and future potential of solar and wind energy over Africa using the RegCM4 CORDEX-CORE ensemble. *Climate Dynamics*, *57*(5), 1647–1672. https://doi.org/10.1007/s00382-020-05377-1

Schär, C., Fuhrer, O., Arteaga, A., Ban, N., Charpilloz, C., Di Girolamo, S., et al. (2020). Kilometer-scale climate models: Prospects and challenges. *Bulletin of the American Meteorological Society*, *101*(5), E567–E587. https://doi.org/10.1175/bams-d-18-0167.1

Scinocca, J., Kharin, V., Jiao, Y., Qian, M., Lazare, M., Solheim, L., et al. (2016). Coordinated global and regional climate modeling. *Journal of Climate*, *29*(1), 17–35. https://doi.org/10.1175/JCLI-D-15-0161.1

Shi, Y., Yu, M., Erfanian, A., & Wang, G. (2018). Modeling the dynamic vegetation–climate system over China using a coupled regional model. *Journal of Climate*, *31*(15), 6027–6049. https://doi.org/10.1175/jcli-d-17-0191.1

Shi, Z., Sha, Y., Liu, X., Xie, X., & Li, X. (2019). Effect of marginal topography around the Tibetan Plateau on the evolution of central Asian arid climate: Yunnan–Guizhou and Mongolian Plateaux as examples. *Climate Dynamics*, *53*(7), 4433–4445. https://doi.org/10.1007/s00382-019-04796-z

Singh, P., & Kumar, N. (1997). Effect of orography on precipitation in the western Himalayan region. *Journal of Hydrology*, *199*(1), 183–206. https://doi.org/10.1016/S0022-1694(96)03222-2

Slingo, A., & Pearson, D. W. (1987). A comparison of the impact of an envelope orography and of a parametrization of orographic gravity-wave drag on model simulations. *Quarterly Journal of the Royal Meteorological Society*, *113*(477), 847–870. https://doi.org/10.1002/qj.49711347708

Smith, R. B. (2019). 100 Years of progress on mountain meteorology research. *Meteorological Monographs*, *59*, 20-21–20-73. https://doi.org/10.1175/amsmonographs-d-18-0022.1

Smith, S. A., Doyle, J. D., Brown, A. R., & Webster, S. (2006). Sensitivity of resolved mountain drag to model resolution for MAP case-studies. *Quarterly Journal of the Royal Meteorological Society*, *132*(618), 1467–1487. https://doi.org/10.1256/qj.05.67

Son, J. H., Seo, K. H., & Wang, B. (2019). Dynamical control of the Tibetan Plateau on the east Asian summer monsoon. *Geophysical Research Letters*, *46*(13), 7672–7679. https://doi.org/10.1029/2019GL083104

Son, J. H., Seo, K. H., & Wang, B. (2020). How does the Tibetan Plateau dynamically affect downstream monsoon precipitation? *Geophysical Research Letters*, *47*(23), e2020GL090543. https://doi.org/10.1029/2020GL090543

Student (1908). The probable error of a mean. *Biometrika*, *6*(1), 1–25. https://doi.org/10.2307/2331554

Taylor, K. E. (2001). Summarizing multiple aspects of model performance in a single diagram. *Journal of Geophysical Research*, *106*(D7), 7183–7192. https://doi.org/10.1029/2000JD900719

Teodoro, T. A., Reboita, M. S., Llopart, M., da Rocha, R. P., & Ashfaq, M. (2021). Climate change impacts on the South American monsoon system and its surface–Atmosphere processes through RegCM4 CORDEX-CORE projections. *Earth Systems and Environment*, *5*(4), 825–847. https://doi.org/10.1007/s41748-021-00265-y

Tiedtke, M. (1996). An extension of cloud-radiation parameterization in the ECMWF model: The representation of subgrid-scale variations of optical depth. *Monthly Weather Review*, *124*(4), 745–750. https://doi.org/10.1175/1520-0493(1996)124<0745:aeocrp>2.0.co;2

Tong, M., Zheng, Z., & Fu, Q. (2022). Evaluation of east Asian Meiyu from CMIP6/AMIP simulations. *Climate Dynamics*, *59*(7), 2429–2444. https://doi.org/10.1007/s00382-022-06218-z

Torma, C., Coppola, E., Giorgi, F., Bartholy, J., & Pongrácz, R. (2011). Validation of a high-resolution version of the regional climate model RegCM3 over the Carpathian Basin. *Journal of Hydrometeorology*, *12*(1), 84–100. https://doi.org/10.1175/2010jhm1234.1

Torres-Alavez, J. A., Glazer, R., Giorgi, F., Coppola, E., Gao, X., Hodges, K. I., et al. (2021). Future projections in tropical cyclone activity over multiple CORDEX domains from RegCM4 CORDEX-CORE simulations. *Climate Dynamics*, *57*(5), 1507–1531. https://doi.org/10.1007/s00382-021-05728-6

Ueno, K., Fujii, H., Yamada, H., & Liu, L. (2001). Weak and frequent monsoon precipitation over the Tibetan Plateau. *Journal of the Meteorological Society of Japan. Ser. II*, *79*(1B), 419–434. https://doi.org/10.2151/jmsj.79.419

Van Niekerk, A., Sandu, I., Zadra, A., Bazile, E., Kanehama, T., Köhler, M., et al. (2020). COnstraining ORographic Drag Effects (COORDE): A model comparison of resolved and parametrized orographic drag. *Journal of Advances in Modeling Earth Systems*, *12*(11), e2020MS002160. https://doi.org/10.1029/2020ms002160

van Niekerk, A., Shepherd, T. G., Vosper, S. B., & Webster, S. (2016). Sensitivity of resolved and parametrized surface drag to changes in resolution and parametrization. *Quarterly Journal of the Royal Meteorological Society*, *142*(699), 2300–2313. https://doi.org/10.1002/qj.2821 van Niekerk, A., & Vosper, S. B. (2021). Towards a more "scale-aware" orographic gravity wave drag parametrization: Description and initial testing. *Quarterly Journal of the Royal Meteorological Society*, *147*(739), 3243–3262. https://doi.org/10.1002/qj.4126

van Niekerk, A., Vosper, S. B., & Teixeira, M. A. C. (2023). Accounting for the three-dimensional nature of mountain waves: Parametrising partial critical-level filtering. *Quarterly Journal of the Royal Meteorological Society*, *149*(751), 515–536. https://doi.org/10.1002/qj.4421

Vosper, S. B., Niekerk, A., Elvidge, A., Sandu, I., & Beljaars, A. (2020). What can we learn about orographic drag parametrisation from high-resolution models? A case study over the Rocky Mountains. *Quarterly Journal of the Royal Meteorological Society*, *146*(727), 979–995. https://doi.org/10.1002/qj.3720

Wallace, J. M., Tibaldi, S., & Simmons, A. J. (1983). Reduction of systematic forecast errors in the ECMWF model through the introduction of an envelope orography. *Quarterly Journal of the Royal Meteorological Society*, *109*(462), 683–717. https://doi.org/10.1002/qj.49710946202

Wang, B., Bao, Q., Hoskins, B., Wu, G., & Liu, Y. (2008). Tibetan Plateau warming and precipitation changes in East Asia. *Geophysical Research Letters*, *35*(14), L14702. https://doi.org/10.1029/2008GL034330

Wang, X., Pang, G., Yang, M., & Wan, G. (2016). Effects of modified soil water-heat physics on RegCM4 simulations of climate over the Tibetan Plateau. *Journal of Geophysical Research: Atmospheres*, *121*(12), 6692–6712. https://doi.org/10.1002/2015JD024407

Wang, Y., Xu, X., Lupo, A. R., Li, P., & Yin, Z. (2011). The remote effect of the Tibetan Plateau on downstream flow in early summer. *Journal of Geophysical Research*, *116*(D19), D19108. https://doi.org/10.1029/2011JD015979

Wang, Y., Yang, K., Zhou, X., Chen, D., Lu, H., Ouyang, L., et al. (2020). Synergy of orographic drag parameterization and high resolution greatly reduces biases of WRF-simulated precipitation in central Himalaya. *Climate Dynamics*, *54*(3–4), 1729–1740. https://doi.org/10.1007/s00382-019-05080-w

Wood, N., Brown, A. R., & Hewer, F. E. (2001). Parametrizing the effects of orography on the boundary layer: An alternative to effective roughness lengths. *Quarterly Journal of the Royal Meteorological Society*, *127*(573), 759–777. https://doi.org/10.1256/smsqj.57302

Wood, N., & Mason, P. (1993). The pressure force induced by neutral, turbulent-flow over Hills. *Quarterly Journal of the Royal Meteorological Society*, *119*(514), 1233–1267. https://doi.org/10.1002/qj.49711951402

Wu, G., Liu, Y., Zhang, Q., Duan, A., Wang, T., Wan, R., et al. (2007). The influence of mechanical and thermal forcing by the Tibetan Plateau on Asian climate. *Journal of Hydrometeorology*, *8*(4), 770–789. https://doi.org/10.1175/JHM609.1

Wu, Z., Zhang, P., Chen, H., & Li, Y. (2016). Can the Tibetan Plateau snow cover influence the interannual variations of Eurasian heat wave frequency? *Climate Dynamics*, *46*(11), 3405–3417. https://doi.org/10.1007/s00382-015-2775-y

Xie, J., Zhang, M., Xie, Z., Liu, H., Chai, Z., He, J., & Zhang, H. (2020). An orographic-drag parametrization scheme including orographic anisotropy for all flow directions. *Journal of Advances in Modeling Earth Systems*, *12*(3), e2019MS001921. https://doi.org/10.1029/2019MS001921

Xie, W., Zhou, B., Han, Z., & Xu, Y. (2021). Projected changes in heat waves over China: Ensemble result from RegCM4 downscaling simulations. *International Journal of Climatology*, *41*(7), 3865–3880. https://doi.org/10.1002/joc.7047

Xin, X., Wu, T., Zhang, J., Yao, J., & Fang, Y. (2020). Comparison of CMIP6 and CMIP5 simulations of precipitation in China and the East Asian summer monsoon. *International Journal of Climatology*, *40*(15), 6423–6440. https://doi.org/10.1002/joc.6590

Xu, X., Li, R., Teixeira, M. A. C., & Lu, Y. (2021). On the momentum flux of vertically propagating orographic gravity waves excited in nonhydrostatic flow over three-dimensional orography. *Journal of the Atmospheric Sciences*, *78*(6), 1807–1822. https://doi.org/10.1175/jas-d-20-0370.1

Xu, X., Xue, M., Teixeira, M. A. C., Tang, J. P., & Wang, Y. (2019). Parameterization of directional absorption of orographic gravity waves and its impact on the atmospheric general circulation simulated by the weather research and forecasting model. *Journal of the Atmospheric Sciences*, *76*(11), 3435–3453. https://doi.org/10.1175/Jas-D-18-0365.1

Xue, H., & Shen, X. (2023). A turbulent orographic form drag scheme accounting for anisotropy and orientation for kilometer- to subkilometer-scale models. *Quarterly Journal of the Royal Meteorological Society*, *149*(755), 2527–2549. https://doi.org/10.1002/qj.4519

Xue, H., Zhou, X., Luo, Y., & Yin, J. (2021). Impact of parameterizing the turbulent orographic form drag on convection-permitting simulations of winds and precipitation over South China during the 2019 pre-summer rainy season. *Atmospheric Research*, *263*, 105814. https://doi.org/10.1016/j.atmosres.2021.105814

Yang, H., Jiang, Z., & Li, L. (2016). Biases and improvements in three dynamical downscaling climate simulations over China. *Climate Dynamics*, *47*(9), 3235–3251. https://doi.org/10.1007/s00382-016-3023-9

Yang, M., Yao, T., Gou, X., Wang, H., & Ha, L. (2007). Comparison analysis of the summer monsoon precipitation between northern and southern slopes of Tanggula Mountains, Qinghai-Xizang (Tibetan) Plateau: A case study in summer 1998. *Hydrological Processes*, *21*(14), 1841–1847. https://doi.org/10.1002/hyp.6319

Yang, M., Zuo, R., Wang, L., & Chen, X. (2018). Simulation of land surface climate over China with RegCM4.5: Verification and analysis. *Advances in Meteorology*, *2018*, 1–14. https://doi.org/10.1155/2018/7960908

Yatagai, A., Kamiguchi, K., Arakawa, O., Hamada, A., Yasutomi, N., & Kitoh, A. (2012). APHRODITE: Constructing a long-term daily gridded precipitation dataset for asia based on a dense network of rain gauges. *Bulletin of the American Meteorological Society*, *93*(9), 1401–1415. https://doi.org/10.1175/bams-d-11-00122.1

Yeh, T. (1950). The circulation of the high troposphere over China in the winter of 1945–46. *Tellus*, *2*(3), 173–183. https://doi.org/10.1111/j.2153-3490.1950.tb00329.x

Yu, E., Wang, H., & Sun, J. (2010). A quick report on a dynamical downscaling simulation over China using the nested model. *Atmospheric and Oceanic Science Letters*, *3*(6), 325–329. https://doi.org/10.1080/16742834.2010.11446886

Zadra, A., Roch, M., Laroche, S., & Charron, M. (2003). The subgrid-scale orographic blocking parametrization of the GEM model. *Atmosphere-Ocean*, *41*(2), 155–170. https://doi.org/10.3137/ao.410204

Zagrodnik, J. P., McMurdie, L. A., Houze, R. A., & Tanelli, S. (2019). Vertical structure and microphysical characteristics of frontal systems passing over a three-dimensional coastal mountain range. *Journal of the Atmospheric Sciences*, *76*(6), 1521–1546. https://doi.org/10.1175/jas-d-18-0279.1

Zeng, X., Zhao, M., & Dickinson, R. E. (1998). Intercomparison of bulk aerodynamic algorithms for the computation of sea surface fluxes using TOGA COARE and TAO data. *Journal of Climate*, *11*(10), 2628–2644. https://doi.org/10.1175/1520-0442(1998)011<2628:iobaaf>2.0.co;2;2

Zhang, Q., Xu, C.-Y., Zhang, Z., Chen, Y. D., Liu, C.-L., & Lin, H. (2008). Spatial and temporal variability of precipitation maxima during 1960–2005 in the Yangtze River basin and possible association with large-scale circulation. *Journal of Hydrology*, *353*(3), 215–227. https://doi.org/10.1016/j.jhydrol.2007.11.023

Zhang, R., Xu, X., & Wang, Y. (2020). Impacts of subgrid orographic drag on the summer monsoon circulation and precipitation in East Asia. *Journal of Geophysical Research: Atmospheres*, *125*(13). https://doi.org/10.1029/2019JD032337

Zhang, Y., Zhang, F., & Sun, J. (2014). Comparison of the diurnal variations of warm-season precipitation for East Asia vs. North America downstream of the Tibetan Plateau vs. the Rocky Mountains. *Atmospheric Chemistry and Physics*, *14*(19), 10741–10759. https://doi.org/10.5194/acp-14-10741-2014

Zhao, C., Jiang, Z., Sun, X., Li, W., & Li, L. (2020). How well do climate models simulate regional atmospheric circulation over East Asia? *International Journal of Climatology*, *40*(1), 220–234. https://doi.org/10.1002/joc.6205

Zhao, C., Xu, M., Wang, Y., Zhang, M., Guo, J., Hu, Z., et al. (2019). Modeling extreme precipitation over East China with a global variable-resolution modeling framework (MPASv5.2): Impacts of resolution and physics. *Geoscientific Model Development*, *12*(7), 2707–2726. https://doi.org/10.5194/gmd-12-2707-2019

Zhao, Y., Chen, D., Li, J., Chen, D., Chang, Y., Li, J., & Qin, R. (2020). Enhancement of the summer extreme precipitation over North China by interactions between moisture convergence and topographic settings. *Climate Dynamics*, *54*(5–6), 2713–2730. https://doi.org/10.1007/s00382-020-05139-z

Zhao, Y., Xu, X., Ruan, Z., Chen, B., & Wang, F. (2019). Precursory strong-signal characteristics of the convective clouds of the Central Tibetan Plateau detected by radar echoes with respect to the evolutionary processes of an eastward-moving heavy rainstorm belt in the Yangtze River Basin. *Meteorology and Atmospheric Physics*, *131*(4), 697–712. https://doi.org/10.1007/s00703-018-0597-2

Zhong, S., & Chen, Z. (2015). Improved wind and precipitation forecasts over South China using a modified orographic drag parameterization scheme. *Journal of Meteorological Research*, *29*(1), 132–143. https://doi.org/10.1007/s13351-014-4934-1

Zhou, T.-J., & Yu, R.-C. (2005). Atmospheric water vapor transport associated with typical anomalous summer rainfall patterns in China. *Journal of Geophysical Research*, *110*(D8), D08104. https://doi.org/10.1029/2004JD005413

Zhou, X., Beljaars, A., Wang, Y., Huang, B., Lin, C., Chen, Y., & Wu, H. (2017). Evaluation of WRF Simulations with different selections of subgrid orographic drag over the Tibetan Plateau. *Journal of Geophysical Research-Atmospheres*, *122*(18), 9759–9772. https://doi.org/10.1002/2017jd027212

Zhou, X., Yang, K., Beljaars, A., Li, H., Lin, C., Huang, B., & Wang, Y. (2019). Dynamical impact of parameterized turbulent orographic form drag on the simulation of winter precipitation over the western Tibetan Plateau. *Climate Dynamics*, *53*(1–2), 707–720. https://doi.org/10.1007/s00382-019-04628-0

Zou, J., & Xie, Z. (2012). The effects of the land-surface process parameterization of the RegCM4 on climate simulation in East Asia. *Acta Meteorologica Sinica*, *70*(6), 1312–1326. https://doi.org/10.11676/qxxb2012.110

Zou, L., & Zhou, T. (2017). Dynamical downscaling of East Asian winter monsoon changes with a regional ocean–atmosphere coupled model. *Quarterly Journal of the Royal Meteorological Society*, *143*(706), 2245–2259. https://doi.org/10.1002/qj.3082